8-2012

A Study on Conformal Antenna Solutions for Cube Satellites

Maryam Jamali
Utah State University

A STUDY ON

CONFORMAL ANTENNA SOLUTIONS FOR CUBE SATELLITES

by

Maryam Jamali

A thesis submitted in partial fulfillment
of the requirements for the degree

of

MASTER OF SCIENCE

in

Electrical Engineering

Approved:

Dr. Reyhan Baktur Major Professor	Dr. Doran Baker Committee Member
Dr. Jacob Gunther Committee Member	Dr. Mark R. McLellan Vice President for Research and Dean of the School of Graduate Studies

UTAH STATE UNIVERSITY
Logan, Utah

2012

Abstract

A Study on

Conformal Antenna Solutions for Cube Satellites

by

Maryam Jamali, Master of Science

Utah State University, 2012

Major Professor: Dr. Reyhan Baktur
Department: Electrical and Computer Engineering

This master's thesis presents a study on a slot and microstrip patch as the two main types of antennas for the use on Cube Satellite (CubeSat). A study on the fundamentals of the slot antenna is researched and a circularly polarized (CPd) cavity-backed cross slot antenna and its two-element array for the CubeSat are designed and fabricated. Fabricated two-element phased array cross slot antenna has higher radiation gain and steered radiation pattern compared to the fabricated single cross slot antenna. A CPd square microstrip patch antenna for the application of the CubeSat is designed and compared with a commercial CPd microstrip patch antenna. It is concluded that our designed microstrip patch antenna has a better performance compared to the commercial one. The last part of the research focuses on the design of miniaturized slot antennas for the CubeSat working at an ultra high frequency (UHF) band. The different techniques and challenges that we face through the miniaturization are articulated throughout the research and expanded upon in this thesis.

The antenna simulations were performed using Ansoft High Frequency System Simulator (HFSS) and the final designs for the CPd cavity-backed single and two-element cross slot antennas and CPd microstrip patch antenna were fabricated using a circuit board milling

machine. These were then measured inside an anechoic chamber for the radiation pattern. Both antennas had high radiation gain and good CPd radiation quality.

(90 pages)

Public Abstract

A Study on

Conformal Antenna Solutions for Cube Satellites

by

Maryam Jamali, Master of Science

Utah State University, 2012

Major Professor: Dr. Reyhan Baktur
Department: Electrical and Computer Engineering

This master's thesis presents a study on two types of conformal antennas for the use on cube satellites (CubeSats). The two antenna solutions are including slot and microstrip patch antennas. CubeSats have been one of the most important vehicles for space exploration due to their small sizes and very low payload. At the same time, a challenge rises when allocating extremely limited surface real estate to space instrument, solar cells, and antennas. The most effective solution for such a challenge is to design antennas such that they do not block solar cells or compete for space with solar cells. Accordingly, antennas with slot geometry is an effective solution because slot antennas can be places around solar cells and the slots are narrow enough to be fit into the spaces between solar cells. This thesis presents detailed studies of slot antennas with different frequencies, single and array configurations. Circular polarization is a favored character for satellite antennas used and it requires specific antenna geometry together with appropriate feeding network design. Design of circularly polarized slot antennas in single and array configurations is one of the main objectives of this thesis research. In order to compare the performance of a slot a patch antenna, a patch with the same polarization and operational frequency has been designed. It shows that if integration with solar cells is not the restriction, then a patch antenna is a

more effective solution. When patch antenna is employed, however, the antenna can only be placed under the satellite where the surface does not need to place solar cells. The other objective of this study is designing circularly polarized antenna for CubeSat working at an ultra high frequency (UHF) band. As the frequency decreases, the size of the antenna increases, and this requires us to use different miniaturization techniques for the antenna. Some applicable miniaturization techniques and their challenges are addressed in this thesis.

This thesis is dedicated to my loving dad, mom, brother, sister, and my beloved husband who all mean the world to me...

Acknowledgments

My first and foremost gratitude is to my advisor, Dr. Reyhan Baktur, for all her support, encouragement, guidance, and efforts. I would like to thank her because of the opportunity she gave me to follow and accomplish my research interests in her group and I am really grateful for what I learned from her kind-hearted personality. I would like to acknowledge other members of my committee, Dr. Doran Baker and Dr. Jacob Gunther, for their time in helping this thesis become a better product. I offer my sincere acknowledgment to the ECE department head, Dr. Todd Moon, for being very supportive of me to enter the program and pursue my MS degree. I want to thank my colleagues at Utah State University, Tursunjan Yasin and Mangalam Chandak, for their help while I was measuring my antennas. I would like to thank my friends in Logan, especially Leila Ahmadi and Kamelia Ahmadi, for their hospitalities. I am extremely grateful for my wonderful family, especially my parents, for their endless love and selfless efforts throughout my whole life. I would like to thank my in-laws for their support, love, and prayers. Finally, I have to thank my other half, my lovely husband, Ali. Without his help I could not follow my goals. His support cannot be more appreciated.

Maryam Jamali

Contents

List of Tables

List of Figures

Chapter 1

Introduction

A CubeSat, a $10\,cm \times 10\,cm \times 10\,cm$ cube, in a category of small satellites is one of the most fitting devices for space communication due to its small size, low payload, and capability of collecting the data from multiple points [1]. Satellites with less than 500 kg wet mass (including fuel) are called small satellites. A 2U sat ($10\,cm \times 10\,cm \times 20\,cm$) and a 3U sat ($10\,cm \times 10\,cm \times 30\,cm$) that have a volume of twice and three times the CubeSat respectively, are the other two types of small satellites which are used in space. Looking for possible antennas to be mounted on the CubeSat's limited surface area and not to be affected by solar cells coverage has led to the noteworthy research on the slot antennas, microstrip patch, and meshed patch antennas. Both slot and microstrip patch antennas are simple, low-profile, inexpensive, and mechanically robust, which makes them suitable for use on satellites, spacecraft, aircraft, and mobile communication devices [2]. However, slot antennas have the advantage of not occupying a large area on the limited surface area over the patch antennas.

Unidirectional radiation is required in order to have more directivity (directivity of antenna is defined as the ratio of the radiation intensity in a given direction from the antenna to the radiation intensity averaged over all directions. Also maximum gain of antenna is defined as the ratio of maximum directivity of antenna divided by antenna efficiency [2]); it can be produced by placing a cavity or a reflector on the back side of the antenna. Another advantage of using a cavity on the back side of the antenna is that it increases the efficiency of the antenna [2]. The cavity can annihilate the surface waves which are caused by increasing the thickness of the substrate for the purpose of antenna bandwidth enhancement. The surface waves degrade the antenna's radiation pattern by extracting power from the total available power for radiation. They travel within the substrate and

they are scattered at bends and surface discontinuities. By using a cavity these surface waves can be eliminated while keeping a large bandwidth [2].

Circular polarization (CP) is a favored polarization for antennas used for satellite communication. In a circularly polarized (CPd) antenna, the electric field varies in two orthogonal planes (X-direction and Y-direction) with the same magnitude and a 90 degree phase difference. The quality of the CP is commonly quantified and expressed as the axial ratio (AR). For a perfect CP the ideal AR value is $0\,dB$, but usually a $3\,dB$ AR is sufficient for most applications. Another method for judging the quality of CP is using co-polar and cross-polar radiation patterns. The co-polar radiation pattern is the radiation pattern of the desired polarization and the cross-polar radiation pattern is the radiation pattern of the undesired opposite polarization [2]. The minimum difference of $15\,dB$ between co-polar and cross-polar components in the direction of maximum directivity is acceptable for an antenna to be considered as a CPd antenna.

Square-shaped slots, cross slots, and circular-shaped slots are structures which can be CPd radiators when an appropriate feed for excitation is chosen [3–5]. Microstrip line, stripline, coplanar waveguide (CPW), and coaxial probe feed are four different types of feeding method for slot antennas [2]. A microstrip line, a conductor with specific width printed on a thin grounded dielectric substrate, is a dispersive transmission line, which means that signals with different frequencies travel with different speeds on it [6]. A microstrip line cannot support a pure transverse electromagnetic (TEM) field because some of its field lines are in the dielectric region and some are in the air [6]; therefore, they have different phase velocities. A stripline, a thin conducting strip with a specific width placed between two wide conductive ground planes with their entire region filled with a dielectric, is a TEM transmission line and is non-dispersive and has no cut-off frequency [6]. CPW has the advantage of lower radiation loss and lower dispersion which makes it more suitable for an array antenna [7], but it has lower effective permittivity compared to the stripline since part of its field is in the air [6]. Exciting the antenna with the coaxial probe feed is easy to fabricate and match but it has a narrow impedance bandwidth [2].

Parts of our objectives in this research were designing CPd slot and patch antennas for the 1U CubeSat to have resonant frequencies in S-band ($2\,GHz$-$4\,GHz$). To have better understanding of slot antennas we studied the effect of the geometry of a slot antenna and a CPd cavity-backed cross slot on their radiation characteristics, which are discussed in the second chapter of this thesis. We chose a cavity-backed cross slot antenna because cross slot has a capability of being CPd antenna, if an appropriate feeding method is designed for it. To the best of my knowledge, there has not been performed many studies on CPd cavity-backed cross slot antennas. Design and fabrication procedures for a CPd cavity-backed cross slot antenna fed with a stripline and its two-element array for the CubeSat are presented in the third chapter. As the other appropriate antenna for CubeSat, we designed a CPd square patch antenna. Although patch antennas are not optimal when been placed on the solar panel, they can be placed on the bottom side of the CubeSat depending on missions and communication requirements. Design and fabrication procedures for a CPd patch antenna for the CubeSat are explained and its performance is compared with the CPd cavity-backed cross slot and a commercial CPd patch antenna in the fourth chapter.

The other part of our objectives was designing CPd UHF slot antennas for two different orientations of the 3U CubeSat in orbit to have resonant frequencies near $350\,MHz$. The UHF band includes frequencies of electromagnetic waves in the range of $300\,MHz$ - $3\,GHz$ and a free space wavelength in the range of $1\,m$ - $10\,cm$, respectively [2]. The design of antennas working at low frequencies for satellite communication is a subject of interest because electromagnetic waves face lower atmospheric loss in space for the lower frequencies or in other words for higher wavelengths. Therefore, the size of the antenna, which has a relation to the wavelength, should be increased, but due to the bounded plane, miniaturization techniques have to be considered to reduce the required area for the antenna. Decreasing the size of the antenna deteriorates its efficiency, impedance bandwidth and AR [8, 9]. By understanding the fundamentals of how a slot antenna works, some research in communication system areas have been done to improve the antenna's radiation characteristics, such as bandwidth and efficiency while miniaturization is a main concern [10–12].

The challenge of the design of the UHF band antenna including the slot antenna for the CubeSat is how to miniaturize the antenna on such a limited surface area while expecting reasonable antenna gain and CPd radiation. So far, only a few studies have been done on designing the miniaturized UHF band antennas [12, 13]. Usually, reported antenna gain for the miniaturized UHF band antennas is less than 2 dB. The objective of this work is to provide an antenna design with high gain, CP, small size and conformal to the CubeSat Surface. A study on high-gain CPd UHF slot antennas for two different orientations of the 3U sat in orbit is presented in the fifth chapter. Finally, possible future studies are addressed in the sixth chapter.

Chapter 2

Investigation of the Effect of the Geometry of the Slot and Cavity-Backed Slot Antennas

2.1 Introduction

The fact that a slot antenna on an infinite ground plane is a complement of the dipole antenna was brought up by H.G. Booker [14]. The slot antenna is a magnetic dipole antenna. Compared with the electric dipole antenna, the polarization of the slot is rotated by 90 degrees and the E-plane and H-plane are swapped [14]. Therefore, unlike the dipole antenna, if a slot is vertical, its polarization is horizontal, and if it is horizontal, it thus results that the polarization will be vertical. Electric current has its maximum amplitude at both of the slot's edges and is zero at the center of the slot [14]. Electric voltage is also at maximum magnitude at the center and is zero at the edges of the slot. Both voltage and current distributions are continuous and sinusoidal, so the impedance is continuous and it increases from zero at the slot's edges to its maximum value at the center of the slot [14]. Although the length of the slot is half of a wavelength, it does not necessarily mean a slot on a ground plane with air as the antenna's dielectric can resonate at a frequency corresponding to its length. If the size of the ground plane compared to the slot length is not large enough, the slot cannot radiate at the expected frequency with the expected bandwidth and efficiency [15].

2.2 Effect of the Slot Width on the Antenna's Radiation Characteristics

For a slot on a ground plane shown in Fig. 2.1, simulations were performed to see the effect of the slot width and its ground plane size on impedance bandwidth and directivity. A 50Ω coaxial cable was used to excite the slot. Initial dimensions for the slot length and width are $390\,mm$ and $2\,mm$, respectively. The initial ground plane size is $500\,mm \times 200\,mm$. It

is expected that this slot antenna resonates around 370 MHz. The bi-directional radiation pattern of this slot is shown in Fig. 2.2. In the first experiment, all dimensions are fixed except for the slot width. The results in Table 2.1 show that the impedance bandwidth improves by increasing the slot width as expected. Increasing the size of antenna improves the bandwidth [9]. Increasing the width decreases the directivity since the size of the ground plane compared to the size of the slot decreases gradually. Because of the limited space in Table 2.1, W is used for the slot width, F for the resonant frequency, BW for the fractional impedance bandwidth, and D for the directivity.

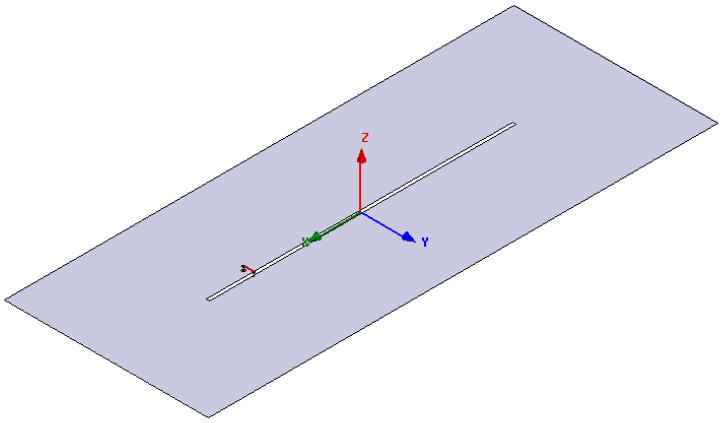

Fig. 2.1: Slot antenna.

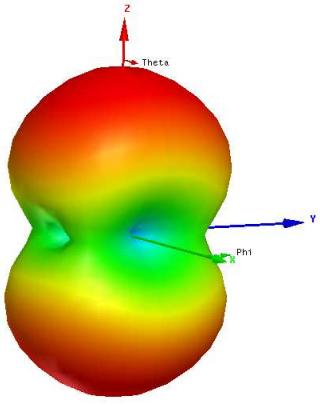

Fig. 2.2: 3-D radiation pattern of the slot antenna.

2.3 Effect of the Ground Plane Dimension on Antenna's Radiation Characteristics

To study the effect of the ground plane size we divided the approach into three different simulations. First, we changed the ground size in a direction, which is in parallel with the slot length (X-direction); second, in a direction perpendicular to the slot length (Y-direction); and third, we increased both sides with the same percentage. When the ground size in the X-direction is increased, the resonant frequency and directivity are both slightly increased and the bandwidth is slightly decreased (Table 2.2). A larger ground plane is a better reflector, which can improve the directivity. However, the reason for reduction in the bandwidth and increase in the frequency is unclear by the time that this thesis is finished. However, these can be subjects of future studies. In Table 2.2, GX is used for the ground size in X-direction and other abbreviations are the same as what were explained for Table 2.1.

Increase in the ground size in the Y-direction increases the impedance bandwidth and slightly decreases the resonant frequency and directivity (Table 2.3). It is expected that enlarging the ground improves the bandwidth and reduces the resonant frequency because currents can circulate around the slot more freely. Although the reduction in the directivity caused by the increase in the ground size in the Y-direction is not significant, its reason at the time that this research is done is unclear and can be a subject for future studies. In this table, GY is used for the ground size in the Y-direction and other abbreviations are the same as what were explained for Table 2.1.

For the last simulations, both ground dimensions ($200mm \times 500mm$) were increased by 10%, 20% and less than 30% to $220mm \times 550mm$, $240mm \times 600mm$, and $260mm \times 650mm$, respectively. The results are shown in Table 2.4. In this table, G is used for the ground dimensions and other abbreviations are the same as what were explained for Table 2.1.

As it is expected, enlarging the ground size decreases the resonant frequency slightly. Also, the directivity and bandwidth both should be improved. This is because of the fact that on a limited ground plane, the electric currents cannot circulate around the slot freely

and as a result the antenna cannot radiate efficiently. Also, a larger ground plane acts as a larger reflector, which can be another reason for improving the directivity. On a larger ground plane the effective wavelength of the electric currents increases, which causes the frequency reduction.

Table 2.1: Effect of the slot width on the impedance bandwidth.

W (mm)	F (MHz)	BW (%)	D (dB)
2	378	1.3	5.73
4	377	4.2	5.61
6	376	5.3	5.57
8	378	6.03	5.35
10	374	6.1	5.17

Table 2.2: Effect of changing the ground size in X-direction on antenna's radiation characteristics.

GX (mm)	F (MHz)	BW (%)	D (dB)
480	372	4.3	5.42
520	377	4.37	5.59
560	378.5	3.9	6.04
600	379	3.4	6.17

Table 2.3: Effect of changing the ground size in Y-direction on antenna's radiation characteristics.

GY (mm)	F (MHz)	BW (%)	D (dB)
200	378	4.1	5.55
220	375	6.9	5.45
240	372	9.4	5.41
260	370	10.2	5.22
280	369	13	5.12

Table 2.4: Effect of the increase in the ground size on antenna's radiation characteristics.

G (mm)	F (MHz)	BW (%)	D (dB)
200×500	378	4.1	5.55
220×550	376	6.9	5.91
240×600	375	8	5.95
260×650	375	9.06	6.19

2.4 Effect of Changing the Dimensions of the Cavity and the Ground Plane of a Cavity-Backed Cross Slot on Antenna's Radiation Characteristics

For many purposes, we want the antenna to radiate only in one direction. Similar to the dipole, slot has a bi-directional radiation. To have unidirectional radiation, a cavity has to be placed on one side of the antenna, which acts like a reflector and suppress the backward radiation. The other advantage of the cavity is eliminating surface waves, which decrease antenna power and efficiency for their radiation [2]. We did another study for the cavity-backed cross slot antenna and for a fixed slot length, to see which dimension has an effect on the resonant frequency. We chose the cavity-backed cross slot antenna shown in Fig. 2.3 for the study. Each slot has $42\,mm$ length and $2\,mm$ width. The cavity is made from metal and the inside of the cavity is filled with a dielectric with relative permittivity of 4.3 and dielectric loss tangent of 0.004. The cross slot antenna is fed with a question mark shape stripline feed sandwiched between two substrates. This feed shape was chosen because of achieving CP and this will be discussed in the next chapter. Each dielectric substrate has $1.524\,mm$ thickness. One of the substrates is inside the cavity and the other is attached to the ground plane, where the cross slot is etched away. The uni-directional radiation pattern of the cavity-backed slot antenna is shown in Fig. 2.4.

To see the effect of the ground we fixed the dimensions of the cavity to $63\,mm \times 63\,mm$ and we changed the size of the ground plane. The results indicate that changing the ground almost does not change the frequency, AR and $3\,dB$ AR bandwidth. It is clear that the size of the ground does not affect radiation so much and this is a desirable property for mobile communication system applications [16]. The results are shown in Table 2.5 and new abbreviations in this table are AR-BW for the $3\,dB$ AR bandwidth and RL for the return loss.

In the second study, the ground dimensions were fixed at $100\,mm \times 100\,mm$ but we changed the dimensions of the cavity behind the cross slot antenna. Decreasing the size of the cavity increases the resonant frequency, efficiency, gain, impedance bandwidth, and AR bandwidth. However, the AR value could be kept almost constant by adjusting

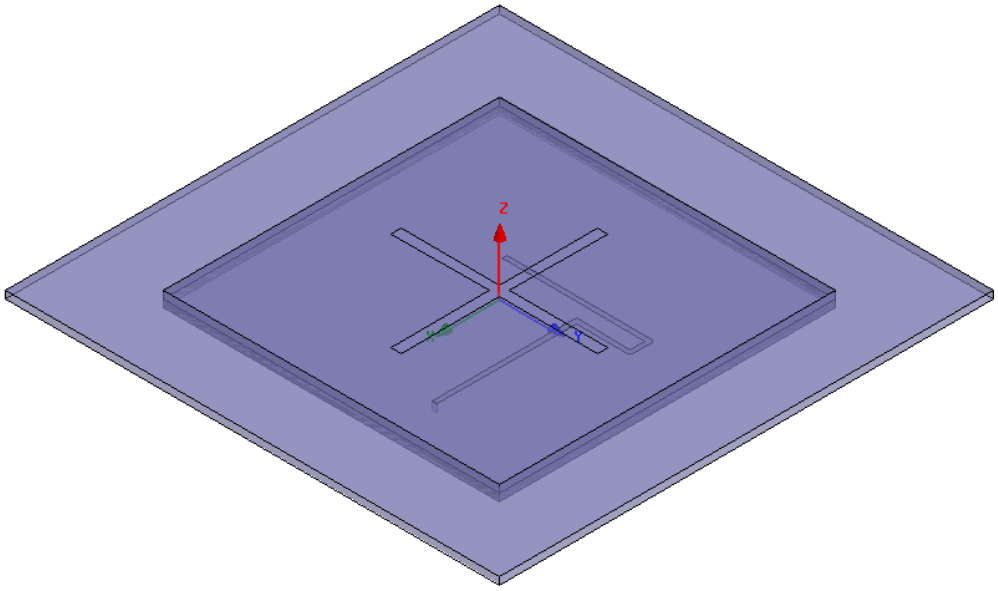

Fig. 2.3: Cavity-backed cross slot antenna.

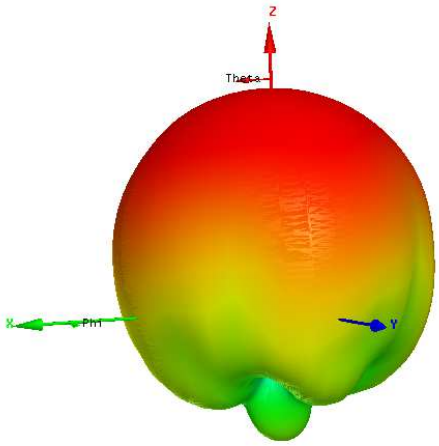

Fig. 2.4: 3-D radiation pattern of the cavity-backed slot antenna.

the position and dimensions of the feed. The resonant frequency is increased because the electric currents are confined in a smaller area. Radiation gain and efficiency are increased because in a smaller cavity currents face less dielectric loss. Decreasing the size of the cavity results in the increase in the impedance bandwidth. The effective ground area is determined by the cavity size. Multiple resonances in adjacent frequency regions can be excited on a smaller ground size, which can be a reason for observing an increase in the bandwidth. The results are shown in Table 2.6. In this table new abbreviations are C for the cavity dimensions, RG for the radiation gain, and E for the radiation efficiency.

Table 2.5: Effect of increasing size of the ground plane on the cavity-backed cross slot antenna's radiation characteristics.

G (mm)	F (MHz)	AR (dB)	AR-BW (MHz)	RL (dB)
70×70	3.48	0.8	25	-10.8
80×80	3.47	0.5	28	-12
90×90	3.48	0.5	28	-13
100×100	3.48	0.3	28	-12

Table 2.6: Effect of decreasing size of the cavity on the cavity-backed cross slot antenna's radiation characteristics.

C (mm)	F (MHz)	AR (dB)	AR-BW (MHz)	BW (MHz)	RG (dB)	E (%)
83×83	2.77	2	12	54.5	4.65	60
78×78	2.91	0.6	19	85	5.69	72
68×68	3.3	0.5	25	98	5.68	77
63×63	3.48	0.6	28	115	5.83	81

Chapter 3

Design and Fabrication of Circularly Polarized Cavity-Backed Cross Slot Antennas: Single and Array Configurations

3.1 Introduction

As mentioned before, a slot antenna is a linearly polarized antenna; therefore, we have to find some techniques for designing appropriate antenna and feed geometries for the CPd radiation. Wong et al. have designed two square and circular printed ring CPd slot antennas [5]. Both circular and square ring slot antennas are excited with a $50-\Omega$ microstrip feed line at an angle of 45 degrees regarding the horizontal axis, and symmetry in both structures is disfigured by protruding one meandered slot section at 45 degrees away from the feed line to excite two electric field components with a phase shift for achieving CP.

The short-circuiting technique was first introduced by Morishita et al. [17]. By short circuiting one point of an annular slot which is 90 degrees away from the feed point, magnetic current distribution changes, which results in achieving CP radiation. This technique was later used by Shi et al. for three different configurations of the cavity-backed slot antennas such as single square loop, two-element square loop and two-arm square spiral slot antennas [18]. In all three structures, the AR varies with the position of the short-circuiting point and the lowest value can be found by moving the short-circuiting point along the slots. A square-ring slot antenna in which its two orthogonal sides are excited with a series microstrip line feed can radiate CP waves [3].

A CP can also be achieved if the proper feeding configuration is used for four slot antennas such that these slots form a square shape and the feed network is designed to

excite these four slots with the same magnitude but different phases of 0 degrees, 90 degrees, 180 degrees, and 270 degrees [19–21].

The cavity-backed cross slot with stripline feed had been designed before [1], but for CP radiation its AR needs to be improved. In this chapter we discuss and compare different designs of the CP cross slot antennas excited by single coaxial feed and stripline feed. Also, fabrication results of the designed CPd cavity-backed cross slot antenna and its two-element array fed by stripline will be compared to their simulation results.

3.2 Circularly Polarized Cavity-Backed Cross Slot Antenna with a Coaxial Feed

For all the single cross slot antennas we chose the ground dimensions to be fitted on a 1U CubeSat. However, to show the effect of the cavity size we also designed the cross slot antenna with a coaxial feed on a ground with the size of 5% larger than a 1U CubeSat size. For all slot antennas, ground and cavity have the same size. We set out to design the slot antennas to resonate between 2.4 GHz and 2.4835 GHz frequency band. It has to be mentioned that the size of the cavity has an effect on the input impedance [4]. If the cavity is too small, the input impedance will be too low because the slot is shorted; and if the cavity is too large, lots of radiating modes will be excited in it and the input impedance varies with frequency too fast, and as a consequence it is hard to match the frequency between two resonating modes.

3.2.1 Circularly Polarized Cavity-Backed Cross Slot Antenna with a Coaxial Feed on the Ground Size of 105 mm×105 mm

First we bring up the design of a cross slot antenna on the ground with a size of $105\,mm \times 105\,mm$ which is a little bit larger than the 1U CubeSat surface area and there is a cavity placed behind it with the same size of the ground and depth of 3.048 mm. For a dielectric inside the cavity we chose two substrates of RO4003C from Rogers Corporation [22] with 3.55 and 0.0027 as its dielectric constant and dielectric loss tangent, respectively. The cross slot is etched on the ground surface and fed with a $50-\Omega$ coaxial probe connected

to the ground surface. Both slots have 2 mm width, but they have different lengths of 43 mm and 46.5 mm. After performing many simulations and looking to the electric current distribution we found that if both slots have equal length, a 90 degree phase shift for CPd radiation cannot be produced. Also, the fact that slots should have different lengths, is mentioned by Sievenpiper et al. [4]. The ground and cavity for generating the same magnitude for phi-component and theta-component of the electric field must have the square shape or circular shape. The difference between the lengths of the slots causes both of them resonate at two adjacent frequencies which also improves the impedance bandwidth. The antenna structure is shown in Fig. 3.1. Position of the probe feed should be found by searching around the cross slot where we have the lowest AR value and return loss of better than -10 dB(Voltage Standing Wave Ratio (VSWR)<2). This antenna has VSWR<2 between the frequencies of 2.416 GHz and 2.48 GHz and has the lowest 0.5 dB AR value at 2.46 GHz shown in Fig. 3.2 and Fig. 3.3, respectively. The fractional impedance bandwidth is about 2.6%. Antenna has the 3dB-CP bandwidth of 10 MHz and the maximum radiation gain of 5.83 dB; the 3-D radiation pattern of the antenna is shown in Fig. 3.4.

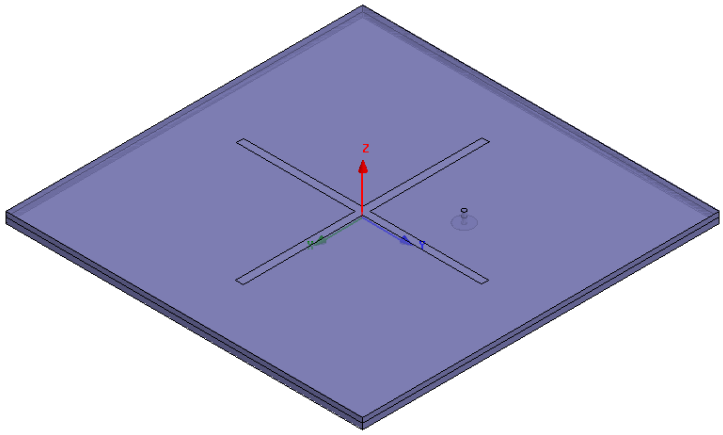

Fig. 3.1: CPd cavity-backed cross slot antenna fed with a coaxial probe.

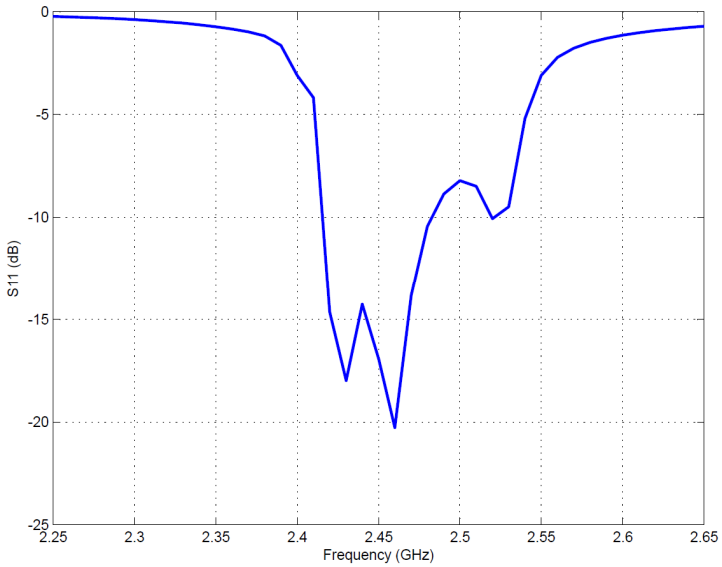

Fig. 3.2: Return loss of the cavity-backed cross slot antenna fed with a coaxial probe.

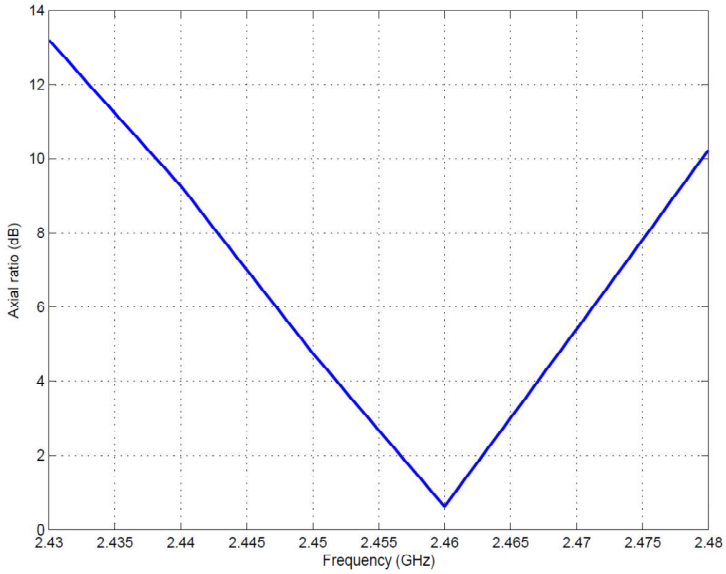

Fig. 3.3: AR of the cavity-backed cross slot antenna fed with a coaxial probe.

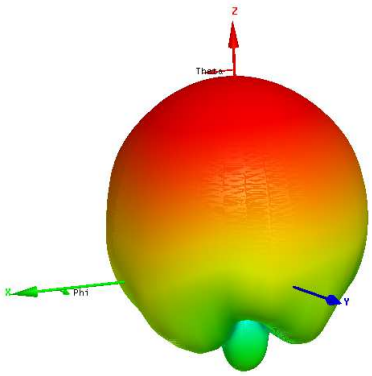

Fig. 3.4: 3-D radiation pattern of the cavity-backed cross slot antenna fed with a coaxial probe.

3.2.2 Circularly Polarized Cavity-Backed Cross Slot Antenna with a Coaxial Feed on the Ground Size of 100 mm×100 mm

In this design the dielectric's specifications and cavity depth are the same as the previous design but this time the cross slot is etched on the ground backed by a cavity with the dimensions of $100\,mm \times 100\,mm$. Because the dimensions of the cavity are reduced by 5% although the slots' lengths are the same as the previous design, the frequency increased to $2.57\,GHz$. Hence, we increased the lengths of the slots to $66.8\,mm$ and $55.5\,mm$ to resonate in the frequency band of our interest while the CPd radiation is a main concern. By performing several parametric studies to find the best position of the probe feed, we achieved the lowest AR value of $1.8\,dB$ at $2.47\,GHz$. For better understanding the effect of the different dimensions of the two designs, the results are compared in Table 3.1. In this table, G is used for the ground dimensions, F for the resonant frequency which has the lowest AR value, BW for the fractional impedance bandwidth, AR-BW for the $3\,dB$ AR bandwidth, and RG for the radiation gain at this resonant frequency. It is observed that by decreasing the cavity size, the impedance bandwidth is reduced and the AR value is increased. Both are because of the fact that the currents around larger slots on a smaller ground cannot circulate freely compared to the previous design which we had smaller slots on a larger ground. The only improvement caused by reducing the dimensions of the cavity

Table 3.1: Effect of the cavity size on the CPd cavity-backed probe-fed cross slot antenna's radiation characteristics.

G (mm)	F (GHz)	BW (%)	AR (dB)	AR-BW (%)	RG (dB)
105×105	2.46	2.6	0.5	0.4	5.83
100×100	2.47	1.53	1.8	0.32	6.41

is related to the lower dielectric loss in the smaller cavity which also was mentioned in the previous chapter.

3.3 Circularly Polarized Cavity-Backed Stripline-Fed Cross Slot Antenna

3.3.1 Design and Simulation Results

To achieve the CPd radiation for the cavity-backed cross slot we chose stripline feed to excite the antenna. In this design, similarly to the previous design, the cavity is filled with two layers of RO4003C with a total thickness of $3.048\,mm$ for the antenna's dielectric. The ground is square of $100\,mm \times 100\,mm$ and crossed slots each with $60\,mm$ length are etched on it to resonate at the frequency in our frequency range of interest. We simulated structures once for the slot with $2\,mm$ width and once for $1\,mm$ width to compare their performances. A $1\,mm$-width stripline feed has a question mark shape and is placed between two substrates in the cavity. The feed shown in Fig. 3.5 has four sections and the length of each section has to be optimized to achieve the CP while antenna is matched, and this causes the design to have a very time consuming procedure. Three edges of stripline feed are tapered to have minimum reflection and maximum transmission. The slot antenna with $2\,mm$ width shown in Fig. 3.6 has a VSWR$<$2 in the frequency range of $2.412\,GHz$ to $2.474\,GHz$ and has the lowest AR value of $0.2\,dB$ at $2.46\,GHz$.

As mentioned above, we also designed a $1\,mm$-width cross slot antenna and we chose this structure for fabrication. It was expected that narrowing the slot would decrease the bandwidth. The return loss of the $1\,mm$-width cross slot antenna is shown in Fig. 3.7. Truncating the length of last section of feed by $1.5\,mm$, which is parallel with Y-axis, was the only adjustment we made to achieve the CP for the narrower slot. The difference

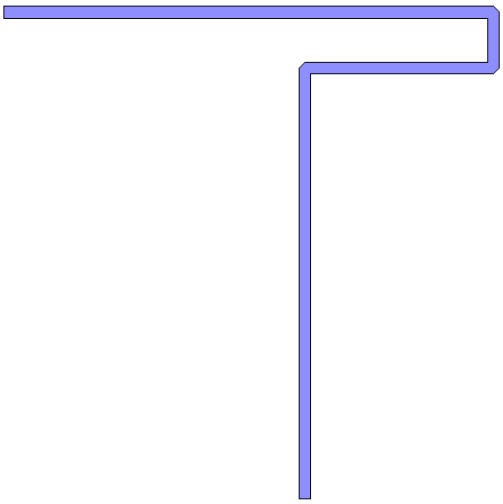

Fig. 3.5: Stripline feed.

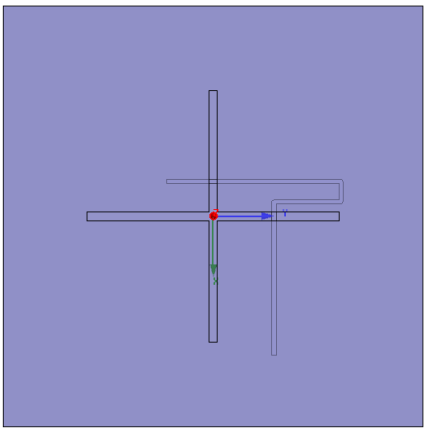

Fig. 3.6: Front view of the cavity-backed stripline-fed cross slot antenna.

between the co-polar and cross-polar components of the radiation pattern at a frequency of 2.42 GHz in the E-plane (Fig. 3.8) and the co-polar and cross-polar components of the radiation pattern in the H-plane (Fig. 3.9) shows that the antenna has CPd radiation at this frequency. Simulation results of both antennas could be found and compared in Table 3.2. In this table, W is used for the slot width and other abbreviations are the same as what

were explained for Table 3.1. If we compare both cross slot antennas fed with a stripline and fed with a single probe feed with the same cavity size and slot width (each is shown in Table 3.1 and Table 3.2), we notice the overall improvement for the antenna when it is fed with a stripline and that is because of the better excitation with the stripline feed.

3.3.2 Fabrication Procedures and Results

We used a circuit board milling machine to fabricate our antennas. As explained in the previous section, we used two dielectric substrates. The stripline feed is etched on one side of one of the substrates and is placed between both substrates. When we measured return loss of the antenna with a network analyzer we noticed a large resonant frequency shift compared to our simulation. The center resonant frequency of the fabricated slot antenna was 2.63 GHz, and as we expected the AR value was not acceptable at this frequency.

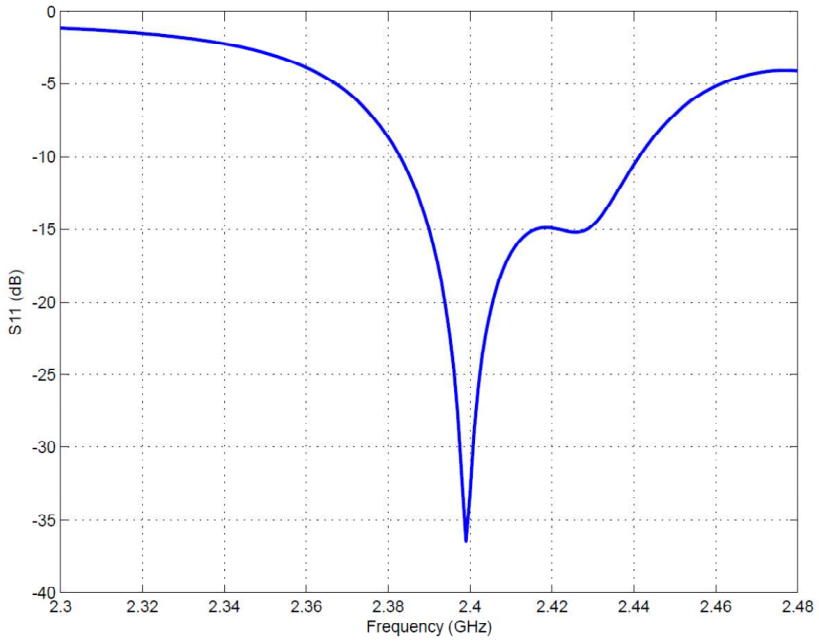

Fig. 3.7: Return loss of the cavity-backed stripline-fed cross slot antenna.

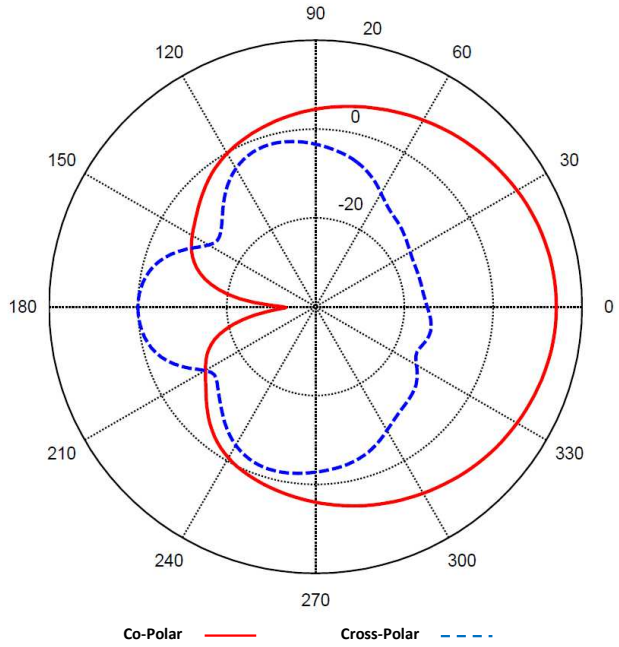

Fig. 3.8: Co-polar and cross-polar components of the radiation pattern in E-plane at 2.42 GHz.

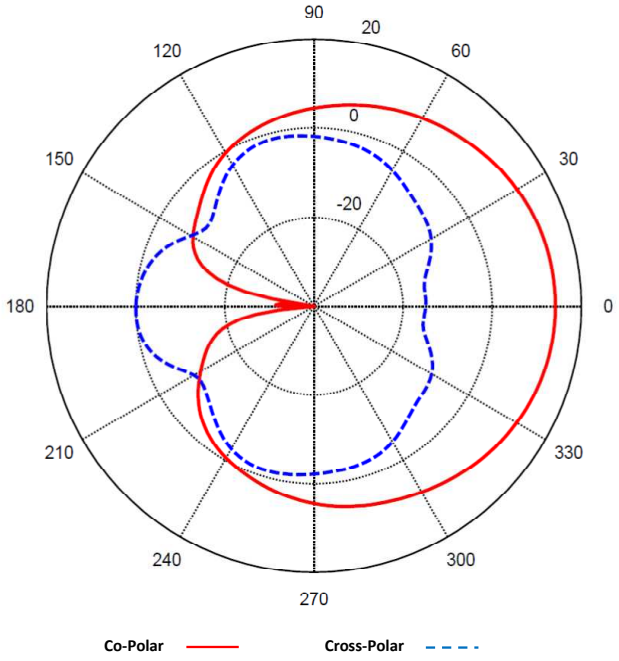

Fig. 3.9: Co-polar and cross-polar components of the radiation pattern in H-plane at 2.42 GHz.

Table 3.2: Radiation characteristics of the stripline-fed cavity-backed cross slot antenna with different slot width.

W (mm)	F (GHz)	BW (%)	AR (dB)	AR-BW (%)	RG (dB)
2	2.46	2.54	0.2	0.7	5.78
1	2.42	2.4	0.6	0.61	5.82

This frequency shift was because of the air gap between two substrates and when we simulated the antenna with the measured air gap between two substrates, simulation results confirmed this frequency shift. To reduce the air gap between dielectric layers we considered fabrication of the second prototype using a few bolts and nuts to attach the two substrates firmly together with more pressure. We simulated the structure with the bolts and nuts to see whether adding these could change antenna's radiation characteristics or not. The simulation results showed if we use the metal bolts and nuts they cause frequency shift but non-metal bolts and nuts do not change the antenna performance. The fabricated antenna with thin plastic bolts and nuts shown in Fig. 3.10 resonates at the center frequency of 2.47 GHz and has a return loss of better than $-10\,dB$ in the frequency band between 2.445 GHz and 2.509 GHz with the fractional impedance bandwidth of 2.59%. Measured return loss and simulated return loss are compared in Fig. 3.11. We used NSI near field range [23] to measure the radiation pattern of the antenna inside an anechoic chamber. The antenna has maximum gain of 5.5 dB at a frequency of 2.48 GHz. By observing the measured co-polar and cross-polar components of the radiation pattern in the E-plane (Fig. 3.12) and the co-polar and cross-polar components of the radiation pattern in the H-plane (Fig. 3.13) at a frequency of 2.48 GHz, we can calculate the AR value in dB by considering the difference between these two values as d using (3.1). Our antenna is a left-hand CPd and has a minimum AR value of $1.66\,dB$. Measured AR is shown in Fig. 3.14.

$$AR\ (dB) = 20\,log\left(\left(1+10^{d/20}\right)/\left(1-10^{d/20}\right)\right) \tag{3.1}$$

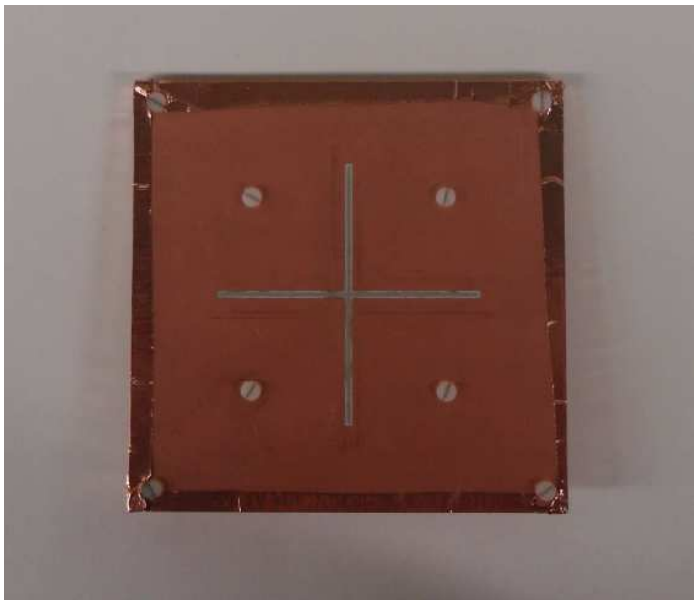

Fig. 3.10: Fabricated CPd cavity-backed stripline-fed cross slot antenna.

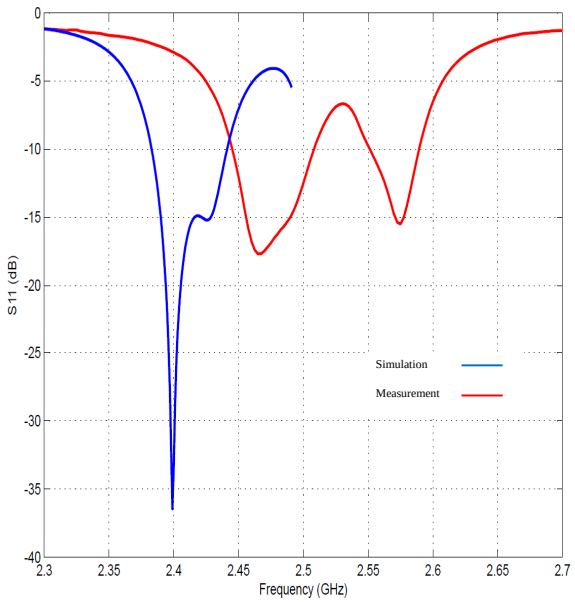

Fig. 3.11: Simulated and measured return loss of the cross slot antenna.

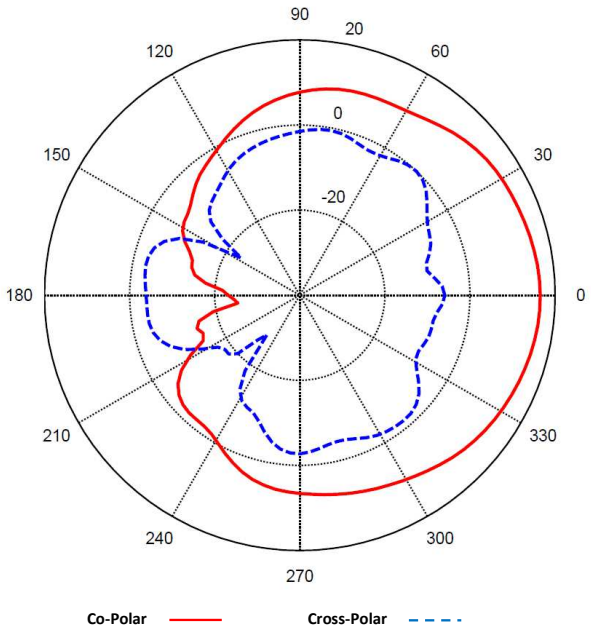

Fig. 3.12: Measured co-polar and cross-polar components of the radiation pattern in E-plane at 2.48 GHz.

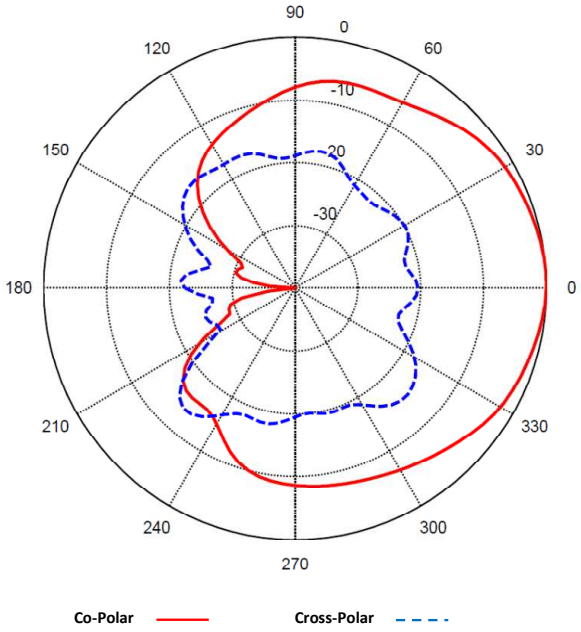

Fig. 3.13: Measured co-polar and cross-polar components of the radiation pattern in H-plane at 2.48 GHz.

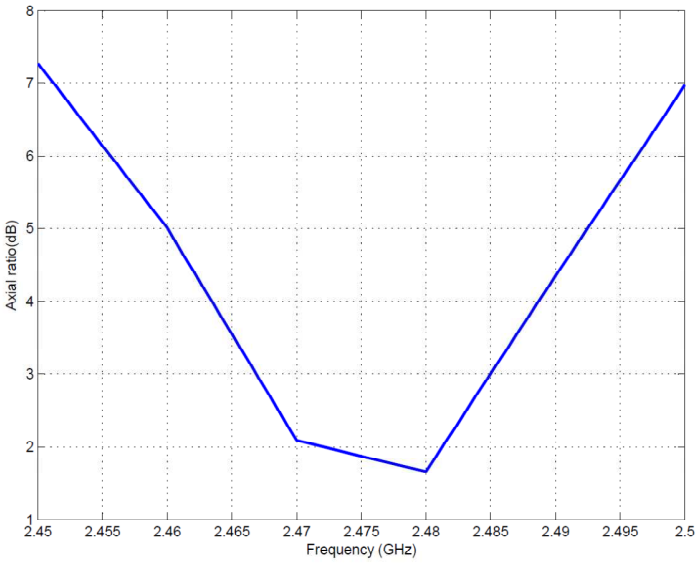

Fig. 3.14: Measured AR of the fabricated cross slot antenna.

3.4 Circularly Polarized Cavity-Backed Stripline-Fed Cross Slot Antenna Array

3.4.1 Design and Simulation Results

To enhance the radiation gain and to steer radiation pattern of the antenna in the desired direction we designed the CPd phased array cross slot antenna shown in Fig. 3.15. Similarly to the cross slot antenna discussed in the previous sections, this array is also a cavity-backed stripline-fed two-element cross slot antenna designed for a 2U CubeSat surface area. The CP can be achieved if individual elements were fed with a phase shift of multiples of 90 degrees [19, 24]. Like the single cross slot antenna, we made two designs of the array with 1 mm and 2 mm slot widths and their simulation results are compared in Table 3.3. The abbreviation in this table is the same as what we used in Table 3.2. It is obvious that the wider array has larger impedance and 3 dB AR bandwidth. The ground size compared to the cross slots is not large enough; therefore, two slots are too close to each other.

So in order to get the antenna to resonate in our frequency band of interest we have to increase the length of slots to 74 mm. To match the antenna with $50 - \Omega$ coaxial probe

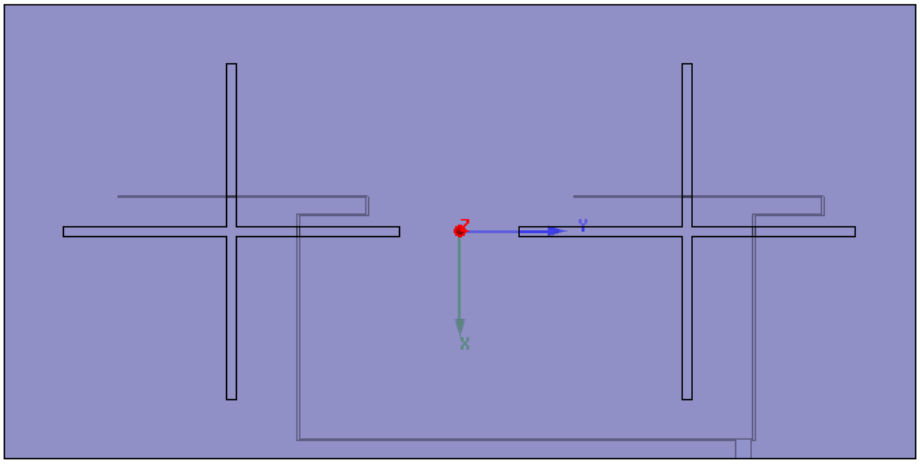

Fig. 3.15: Two-element cross slot antenna array.

we used a T-junction where the coaxial probe connects to the stripline feed. For the slot antenna with 2 mm width, the wide part of the stripline feed has 3.5 mm width, and the two narrow branches have 0.5 mm width. These mentioned dimensions for the width of the stripline feed would be double for the slot with 1 mm width. To apply the phase shift between two elements we used a line phase shifter. The difference between the lengths of the two feeds is 100 mm, which in terms of the phase shift between two elements is a little bit more than 270 degrees. To achieve the CP, the lengths of the different sections of both feeds need to be adjusted even though both feeds have the same dimensions.

Simulations results show that the antenna has a VSWR<2 for the frequencies between 2.38 GHz and 2.505 GHz (Fig. 3.16). Looking to the radiation pattern shown in Fig. 3.17, the beam is steered in two directions because of the limited space between the elements; otherwise the beam is expected to steer in one direction. Antenna is a left-hand CPd with the minimum AR of 0.8 dB at a frequency of 2.48 GHz in θ = -30 degrees and ϕ = -90 degrees direction (Fig. 3.18). The gain of the antenna in this direction is 6.5 dB.

Table 3.3: Radiation characteristics of the two-element array cross slot antenna with different slot width.

W (mm)	F (GHz)	BW (%)	AR (dB)	AR-BW (%)	RG (dB)
2	2.48	5.02	0.8	0.48	6.5
1	2.42	1.65	1.5	0.33	4.86

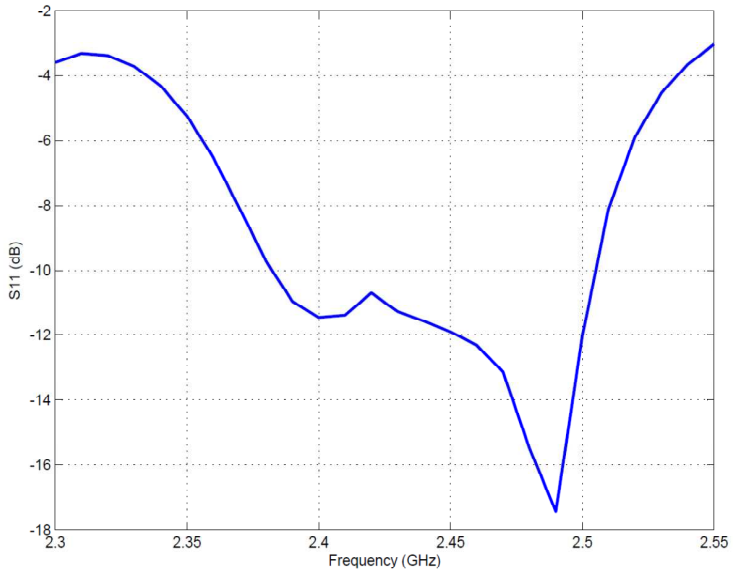

Fig. 3.16: Return loss of the cross slot antenna array.

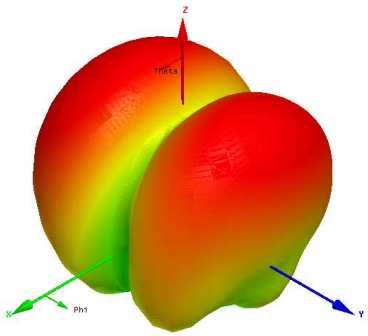

Fig. 3.17: 3-D radiation pattern of the cross slot antenna array.

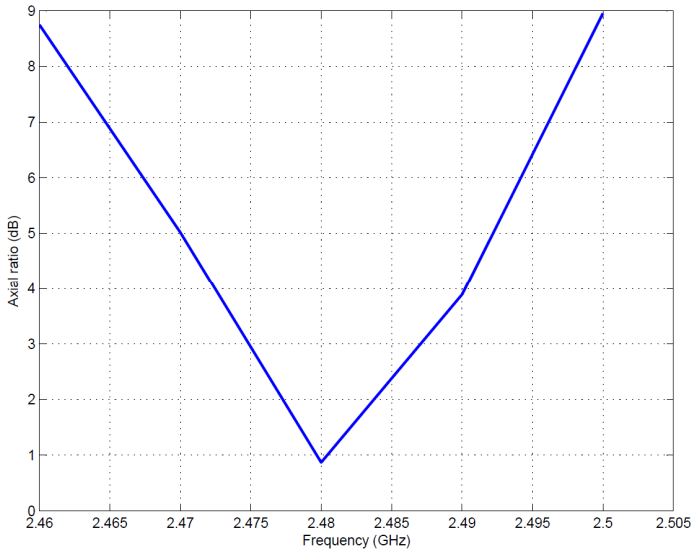

Fig. 3.18: AR of the cross slot antenna array.

3.4.2 Fabrication Procedure and Results

The first prototype of 2 mm-width slot array antenna showed a frequency shift to the frequency band between 2.51 GHz and 2.57 GHz. Therefore, we fabricated the second prototype using plastic bolts and nuts (Fig. 3.19). This antenna has a VSWR<2 for the frequencies between 2.418 GHz and 2.58 GHz. Measured return loss and simulated return loss of the array are compared in Fig. 3.20. The results of the measured radiation pattern of the antenna shows that the antenna has a steered beam with maximum radiation gain of 6.38 dB at a frequency of 2.56 GHz at θ = -14 degrees; however, the gain of the antenna at θ = -21 degrees is very close to the maximum radiation gain. The measured co-polar and cross-polar components of the radiation pattern in the E-plane (Fig. 3.21) and co-polar and cross-polar components of the radiation pattern in the H-plane (Fig. 3.22) show the AR at θ = -14 degrees is 8.6 dB and at θ = -21 degrees is 6.9 dB. The difference between the simulation and fabrication results is due to the precision of the fabrication, which has caused the frequency shift in the fabricated prototype. The antenna array compared to the single antenna is more complex in its structure and requires more precision in its fabrication.

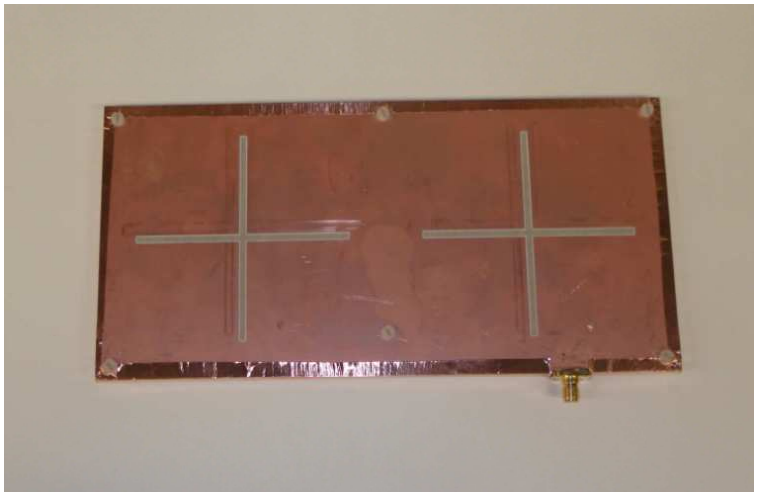

Fig. 3.19: Fabricated cross slot antenna array.

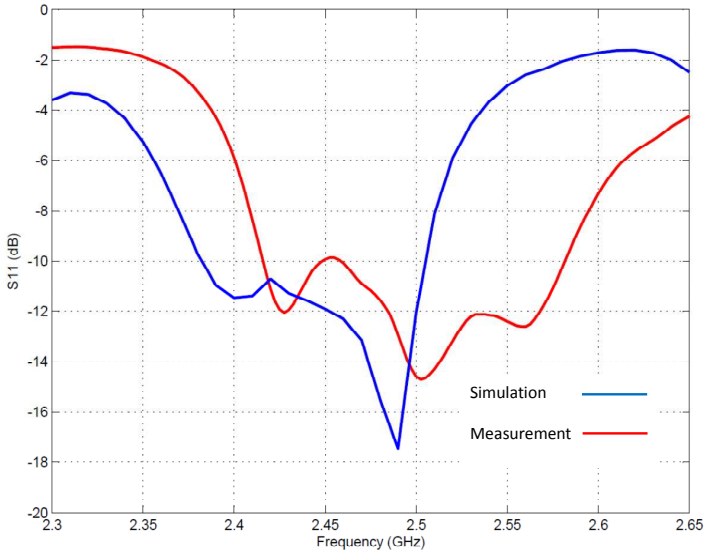

Fig. 3.20: Simulated and measured return loss of the cross slot antenna array.

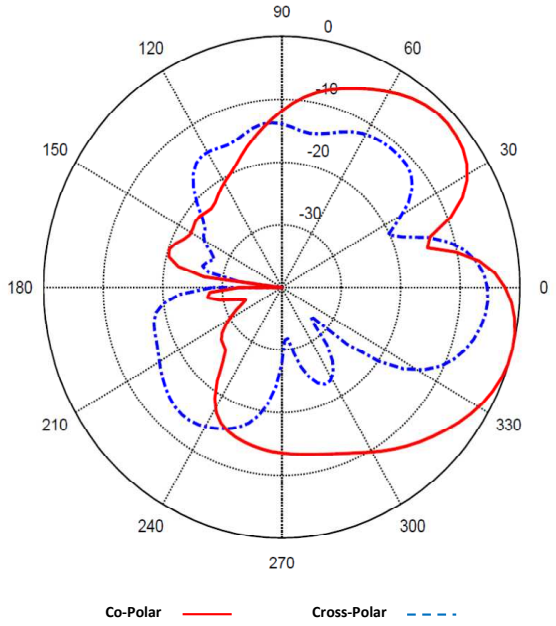

Fig. 3.21: Measured co-polar and cross-polar components of the radiation pattern of the array in E-plane at 2.56 GHz.

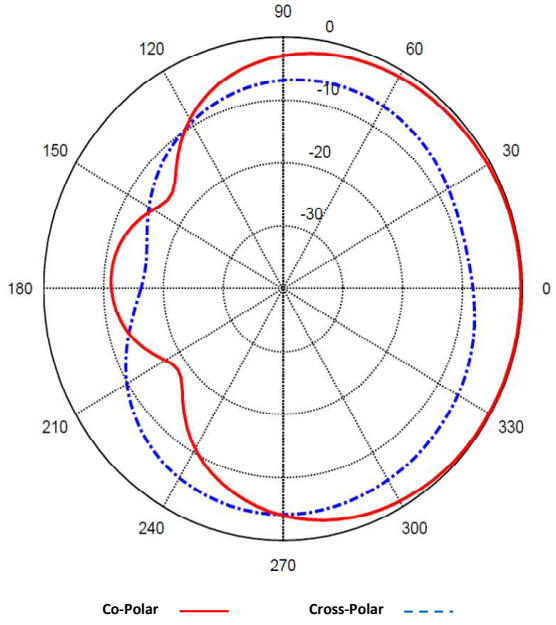

Fig. 3.22: Measured co-polar and cross-polar components of the radiation pattern of the array in H-plane at 2.56 GHz.

Chapter 4

Design and Fabrication of Circularly Polarized Patch Antenna

4.1 Introduction

A microstrip patch is a very common and fitting type of antenna where a low-profile, easy-to-integrate, easy-to-install, and versatile polarized radiation antenna is needed [2]. The patch antenna is a metallic strip placed above the ground plane or usually etched on a dielectric substrate [2]. It can be designed in various shapes, but rectangular patches are the most common configurations. The resonant frequency of the rectangular patch is determined by its length, which is less than a half wavelength [2]. Part of the patch antenna's electric field spreads and closes its path to the ground plane through the edges' fringe, and this makes the electrical length of the patch to be less than its physical length. Microstrip line, coaxial probe, aperture coupling, and proximity coupling are four common feeding methods for exciting the patch antennas [2]. One of the most desired characteristics of the patch antenna is achieving the CPd radiation by creating a asymmetry on the patch or truncating the edges while the antenna is fed with a single coaxial probe [25–27]. Despite mentioned advantages of patch antennas, a narrow impedance bandwidth (which is a fraction of a percent or at most a few percent) can be a drawback for using these antennas [2]. However, there are many applications which do not need wide bandwidth, and therefore patch antennas are appropriate choices to be used. In this chapter we discuss and compare the measurement results of a fabricated square patch antenna fed with a coaxial probe against the results of a commercial patch antenna. We also will compare the performance of the patch antenna with the slot antenna discussed in the previous chapter.

4.2 Design and Simulation Results

We were asked by the Space Dynamics Lab [28] to design a CPd antenna on a ground plane of 80.01 $mm \times 80.01\,mm$ to resonate at a frequency in the frequency band between 2.4 GHz and 2.4835 GHz. SDL has purchased a commercial patch antenna before and we decided to design a patch and compare it with the commercial one and with the designed cavity-backed cross slot antenna to see which one performs better. We designed a 31.9 mm square patch on a RO4003C dielectric substrate with the dielectric constant of 3.55, loss tangent of 0.0027 and thickness of 1.524 mm. We used 50 Ω coaxial probe to feed the patch at the position of 5.75 mm and 0.5 mm off the center in the X-direction and Y-direction, respectively. We truncated two corners of the patch by two equilateral triangles with sides of 2.85 mm for the CP purpose (Fig. 4.1). By truncation, the antenna would have two different lengths in two perpendicular sides and two orthogonal TM_{10} and TM_{01} modes of excitation. We can control the phase difference between two modes by adjusting the lengths of the truncated corners such that two resonant frequencies get close to each other, which causes the impedance bandwidth to get wider while one mode is excited at 90 degrees phase delay with respect to the other mode. Simulation results show that the antenna has the return loss of better than $-10\,dB$ for the frequencies between 2.398 GHz and 2.461 GHz (Fig. 4.2) and has the lowest AR value of 0.8 dB at 2.43 GHz (Fig. 4.3). The maximum radiation gain at this frequency is 7.07 dB (Fig. 4.4).

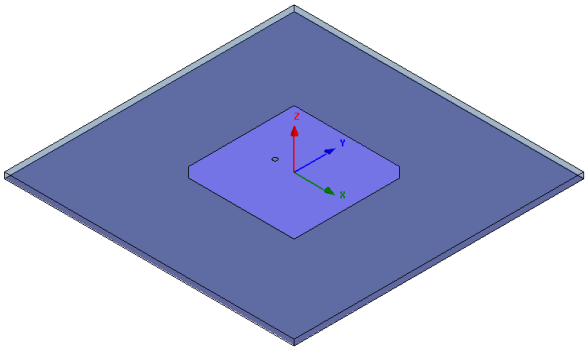

Fig. 4.1: CPd patch antenna.

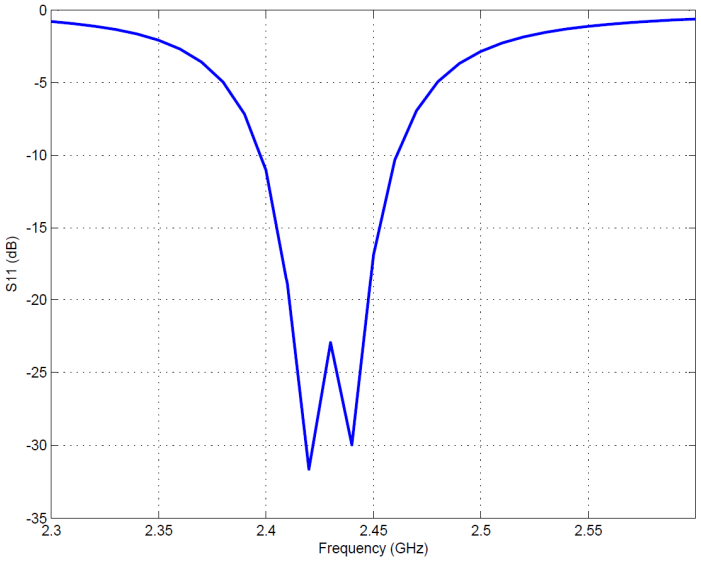

Fig. 4.2: Return loss of the patch antenna.

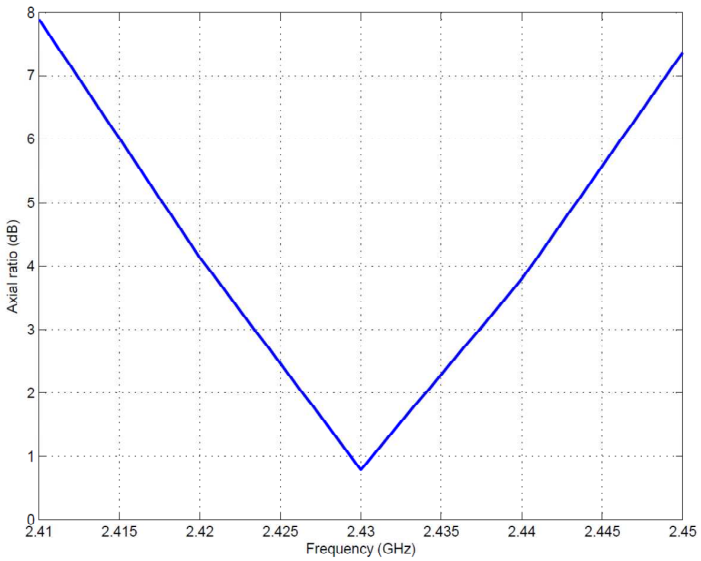

Fig. 4.3: AR of the patch antenna.

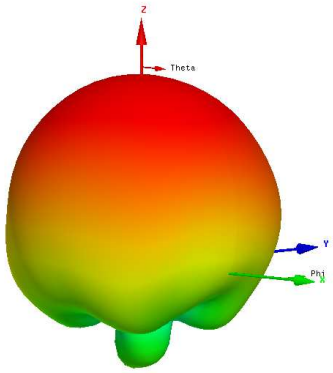

Fig. 4.4: 3-D radiation pattern of the patch antenna.

4.3 Fabrication and Measurement Results

We fabricated the patch antenna by using the circuit board milling machine and we measured its radiation pattern in the anechoic chamber. The antenna shown in Fig. 4.5 has a VSWR<2 for the frequencies between 2.4 GHz and 2.46 GHz, which is equivalent to the 2.47% fractional impedance bandwidth. For better comparison, both measured and simulated return loss are shown in Fig. 4.6. The measured co-polar and cross-polar components of the radiation pattern in the E-plane (Fig. 4.7) and H-plane (Fig. 4.8) show that the antenna is a left hand CPd with a minimum AR value of 0.9 dB at a frequency of 2.425 GHz. The antenna has 6.91 dB gain at this frequency. These results show that there is a very good agreement between simulation and the fabricated prototype.

The commercial patch antenna shown in Fig. 4.9 has a thick dielectric substrate with 6.35 mm thickness; however, the dielectric material is manufacturer's proprietary information. The measured return loss shows that the antenna has a VSWR<2 for the frequencies between 2.436 GHz and 2.51 GHz, which is equivalent to the 2.9% fractional impedance bandwidth (Fig. 4.10). The commercial patch has a wider impedance bandwidth compared to our designed patch and this is because of the larger substrate thickness of the commercial patch antenna. We measured the radiation pattern of the commercial patch for all frequen-

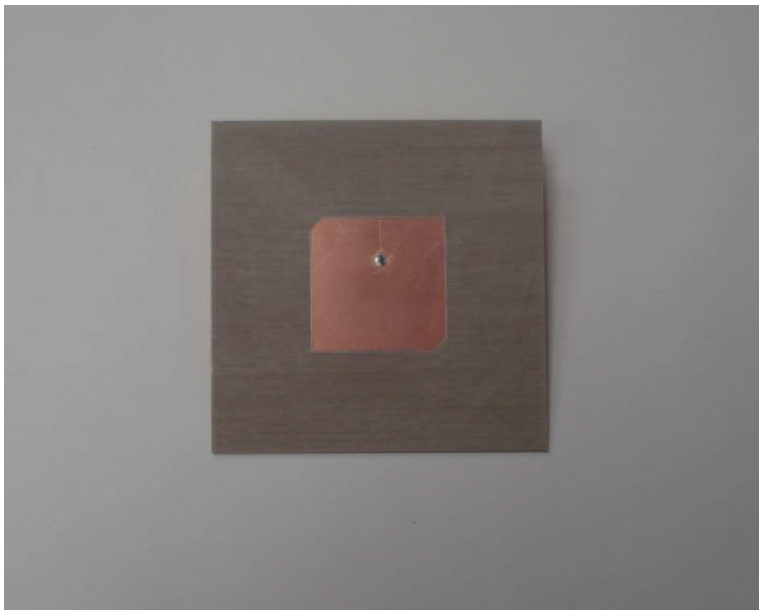

Fig. 4.5: Fabricated patch antenna.

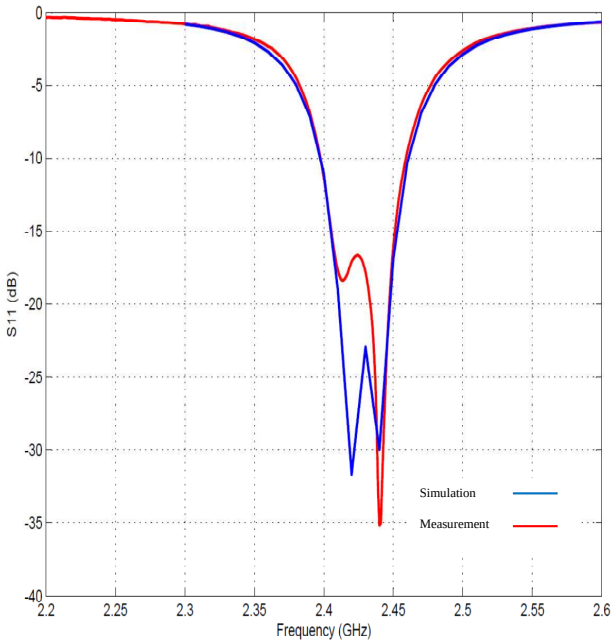

Fig. 4.6: Simulated and measured return loss of the patch antenna.

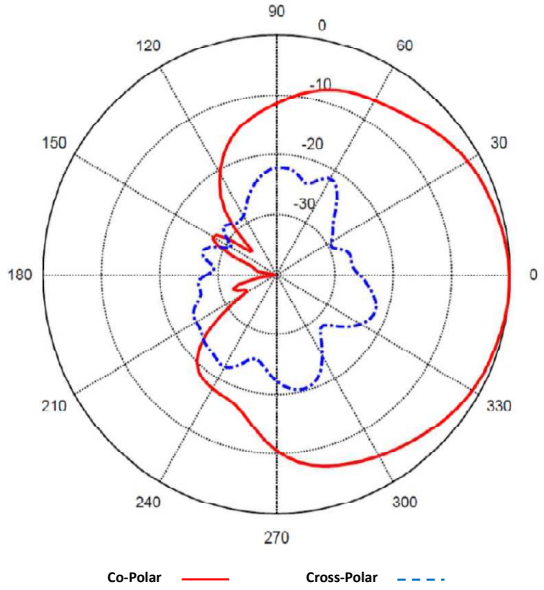

Fig. 4.7: Co-polar and cross-polar components of the patch antenna's radiation pattern in E-plane at 2.425 GHz.

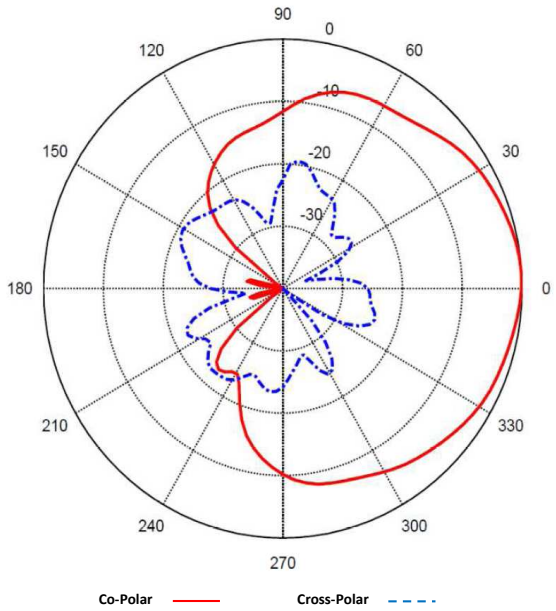

Fig. 4.8: Co-polar and cross-polar components of the patch antenna's radiation pattern in H-plane at 2.425 GHz.

cies of its frequency bandwidth to find its AR value and gain. From the results shown in Table 4.1, we can see that the lowest AR value of the antenna is 3.61 dB at a frequency of 2.48 GHz. These AR values indicate that the commercial patch antenna is not a good CPd radiator. For better visualization of the radiation pattern of the antenna, the co-polar and cross-polar components of the radiation pattern in the E-plane and H-plane at a frequency of 2.48 GHz are shown in Fig. 4.11 and Fig. 4.12, respectively.

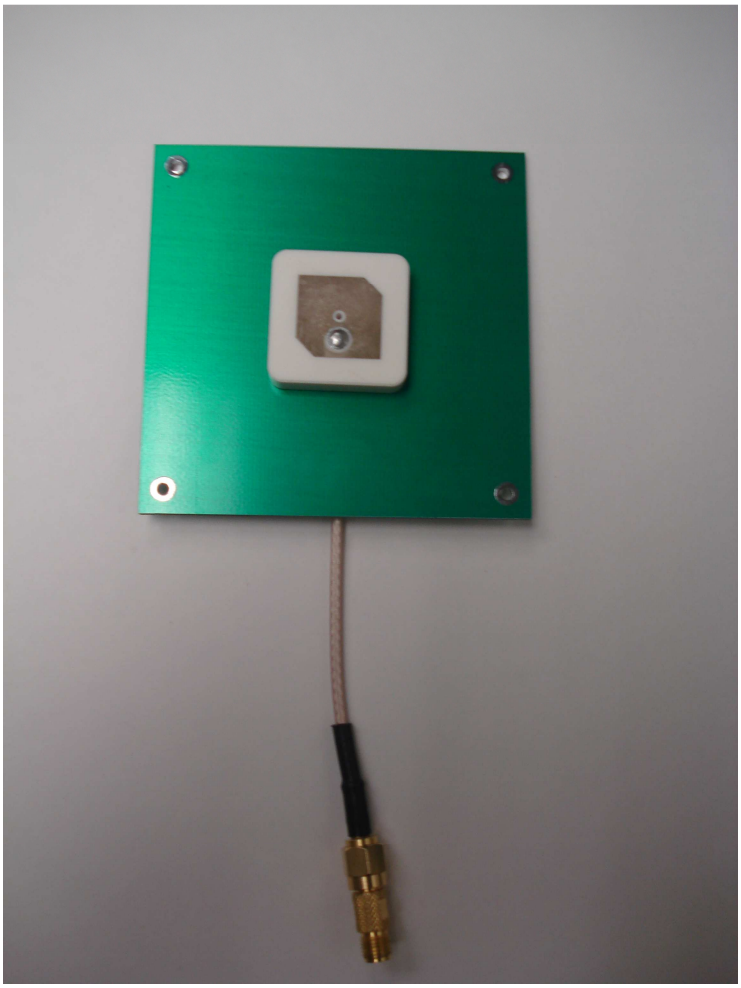

Fig. 4.9: Commercial patch antenna.

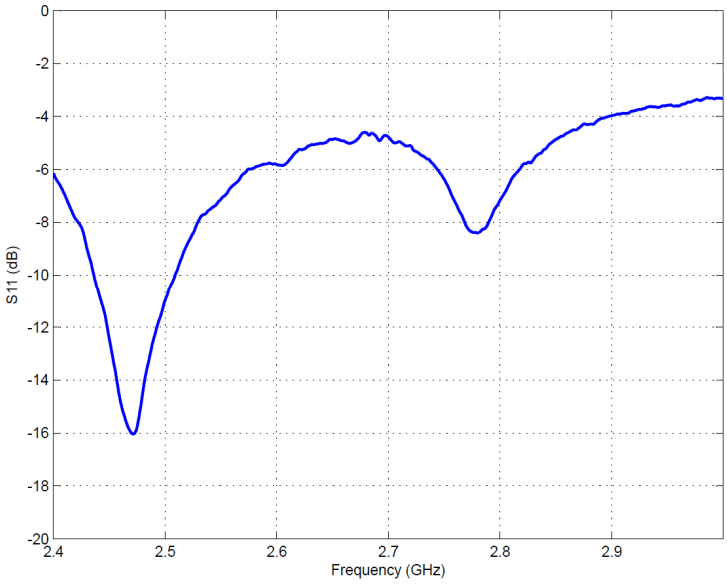

Fig. 4.10: Return loss of the commercial patch antenna.

Table 4.1: Radiation gain and AR values of the commercial patch antenna for various frequencies.

Frequency (GHz)	Gain (dB)	AR (dB)
2.45	6.184	5.4
2.46	6.302	4.4
2.465	6.594	4.09
2.4675	6.543	3.89
2.47	6.579	3.74
2.48	6.93	3.61
2.49	7.2	3.79

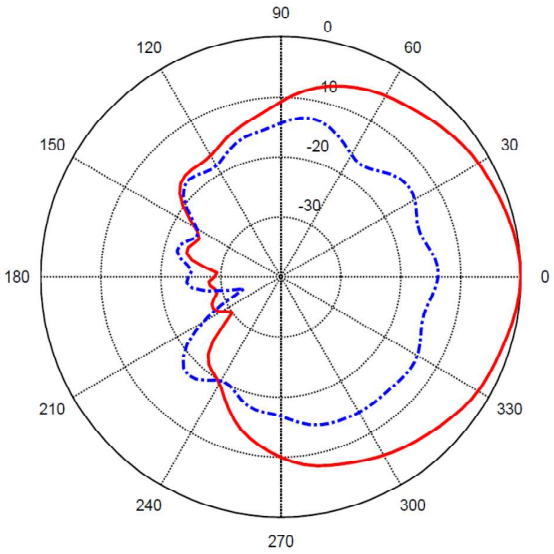

Fig. 4.11: Co-polar and cross-polar components of the commercial patch antenna's radiation pattern in E-plane at 2.48 GHz.

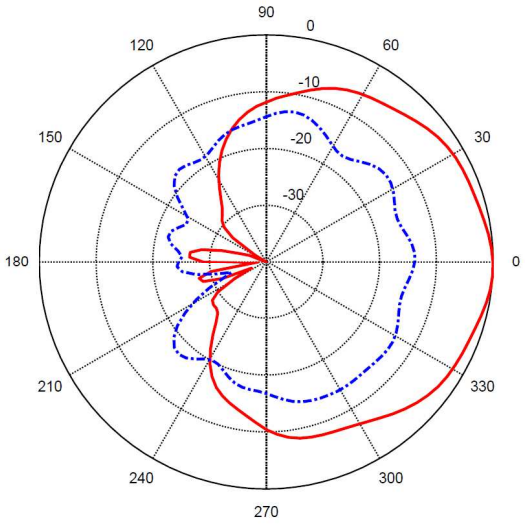

Fig. 4.12: Co-polar and cross-polar components of the commercial patch antenna's radiation pattern in H-plane at 2.48 GHz.

4.4 Patch Antenna Versus Cavity-Backed Cross Slot Antenna

4.4.1 Coaxial Probe-Fed Patch Antenna Versus Coaxial Probe-Fed Cavity-Backed Cross Slot Antenna

To make a valid comparison between performances of the patch antenna and the designed probe-fed cross slot antenna in the previous chapter, we also designed another square patch antenna identical to the one mentioned in the previous sections but on a different ground size of $100\,mm \times 100\,mm$. Both antennas' fractional bandwidth and gain are compared in Table 4.2. It is clear that the patch has larger impedance bandwidth, AR bandwidth, and higher gain.

4.4.2 Coaxial Probe-Fed Patch Antenna Versus Stripline-Fed Cavity-Backed Cross Slot Antenna

We made another comparison between the patch and the cross slot regardless of their feeding methods. We only considered them as two different CPd antennas working at almost the same frequency band. Both antennas have the same ground size of $100\,mm \times 100\,mm$ and slot width of $1\,mm$. Looking to the results in Table 4.3, again it is obvious that the patch has higher gain, larger impedance bandwidth and AR bandwidth.

Table 4.2: Comparison between radiation characteristics of the coaxial probe-fed patch and the coaxial probe-fed cavity-backed cross slot antennas.

Antenna	Impedance bandwidth (%)	AR bandwidth(%)	Gain (dB)
Patch	4.69	1.11	7.26
Cross slot	1.53	0.32	6.41

Table 4.3: Comparison between radiation characteristics of the coaxial probe-fed patch and stripline-fed cavity-backed cross slot antennas.

Antenna	Impedance bandwidth (%)	AR bandwidth(%)	Gain (dB)
Patch	4.69	1.11	7.26
Cross slot	2.4	0.6	5.82

4.4.3 Fabricated Patch Antenna Versus Fabricated Cavity-Backed Cross Slot Antenna

When comparing measured results of the fabricated patch and fabricated cross slot antennas shown in Table 4.4, we conclude that although the slot has lower gain compared to the patch, it has wider bandwidth. However, narrower bandwidth of the patch can be referred to its thinner dielectric substrate and smaller ground plane.

Despite the observed superior performance of the patch antenna over the slot antenna, the main disadvantage of the use of the patch antenna for the CubeSat is that the patch competes for surface area, and this requires us to compromise between the use of the patch and slot antennas for the limited surface area.

Table 4.4: Comparison between radiation characteristics of the fabricated patch and fabricated cavity-backed cross slot antennas.

Antenna	Impedance bandwidth (%)	Minimum AR(dB)	Gain (dB)
Patch	2.47	0.9	6.91
Cross slot	2.59	1.6	5.5

Chapter 5
An Initial Study on High-Gain, Circularly Polarized UHF Slot Antenna

5.1 Introduction

The UHF band in most nations is designated to communication categories like terrestrial television, TV channels, terrestrial radio, and mobile radio service. For UHF band, antenna geometries commonly used are dipole, Yagi-Uda, and loop. These antennas have good performance, however often time come with large sizes. For terrestrial reception usually there is no constraint for antenna sizes. But when used on the satellites, especially small satellites to reduce mission payloads, the large antenna sizes become an issue. It should be noted that the UHF frequency band have been used in various applications such as monitoring space weather, and there are lots of requirements for trasmission power, polarizations, and bandwidths. Trying to satistfy all those requirements while reducing the size of antennas can be challenging. In particular, trying to accommodate all those requirements, size reduction, and having the antenna conformal to solar panel to eliminate expensive deployed mechanism casts extra challenge. The purpose of this chapter is to present some feasibility study of conformal integrated solar panel antennas with high gain and circular polarization for CubeSats.

5.2 Material Selection

All the UHF band slot antennas on the 3U CubeSat have small surface area compared to the antenna size, which increases the electrical current loss and as a result decreases the antenna efficiency. Therefore, we looked for a dielectric with a very small dielectric loss tangent and a moderate dielectric constant. Considering all these, we chose fused quartz

with the relative permittivity of 3.78 and loss tangent of 0.0004 at a frequency of 1 MHz for the dielectric of the antennas in the simulations.

5.3 Simple Slot Antenna

We initially designed a simple slot antenna which is fitted on a 300 $mm \times 100\,mm$ surface area to ascertain the resonant frequency and the gain. We placed a $280\,mm \times 2\,mm$ slot on the ground and fed by a single stripline placed between two dielectric substrates, each of a 2 mm thickness. We expected this slot on the selected dielectric to resonate at a frequency around 275 MHz, but this antenna on the 3U CubeSat ground size resonates at 672 MHz with 5 dB gain. This is because of the limited surface area compared to the antenna size, which does not let the electric current circulate around the slot freely. The antenna, return loss and 3-D radiation pattern are shown in Fig. 5.1, Fig. 5.2, Fig. 5.3, respectively.

5.4 Rectangular-Shaped Slot Antenna on 3U CubeSat

We calculated the required size of the rectangular slot to have a resonant frequency around 350 MHz. For the rectangular- and square-shaped slot antennas the circumference of the slot should be around one wavelength. Thus, for a frequency around 350 MHz at the free space, the perimeter of the rectangular slot should be around 857 mm and on a substrate with a dielectric constant of 3.78, it will be decreased by the effective dielectric constant. A $225\,mm \times 90\,mm$ rectangular-shaped slot antenna with 2 mm width (Fig. 5.4) was chosen; having a total perimeter of 630 mm, it resonates at a frequency of 351 MHz and has the maximum gain of 4.3 dB (Fig. 5.5). Looking at the input impedance of the antenna (Fig. 5.6), it exhibits $170\,\Omega$ impedance. Using a passive matching circuit or active integration with an amplifier can transform it to the standard $50 - \Omega$ systems [29]. If we divide 857 by 630 we reach 1.85 as the effective dielectric constant, which is less than what it should be. The effective dielectric constant is expected to be close to the fused quartz relative permittivity of 3.78 since we use the stripline feed to excite the antenna. Again we have to conclude that it is due to the limited ground size compared to the size of antenna.

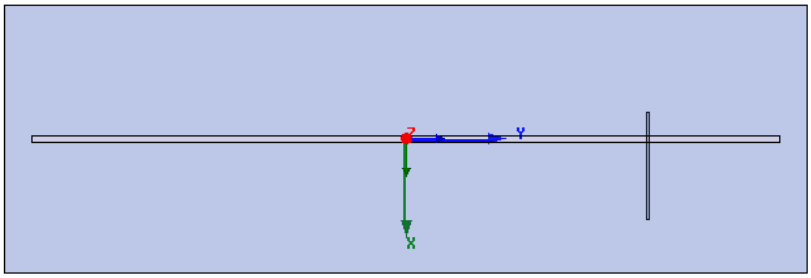

Fig. 5.1: Front view of the simple slot antenna.

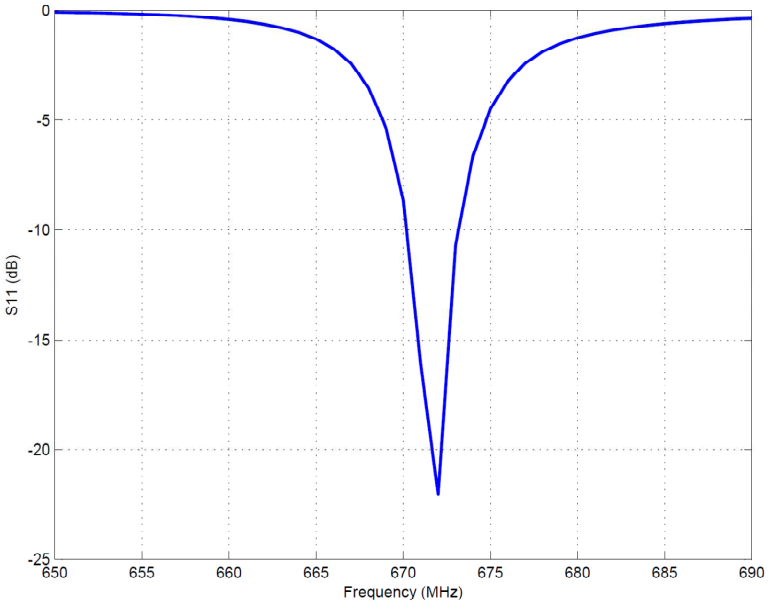

Fig. 5.2: Return loss of the simple slot antenna.

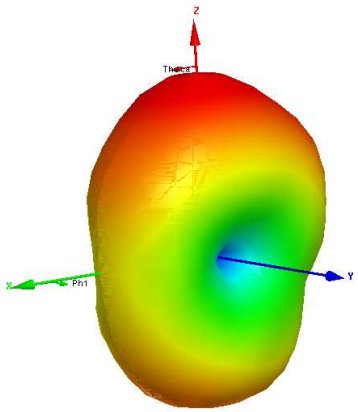

Fig. 5.3: Radiation gain of the simple slot antenna.

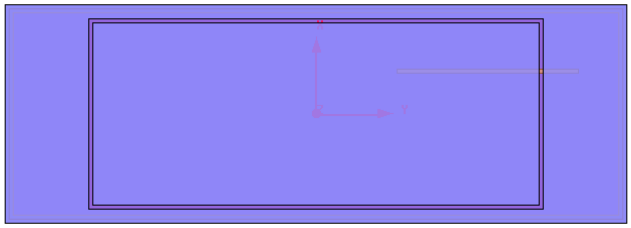

Fig. 5.4: Front view of the rectangular slot antenna.

Although with one rectangular slot we can have resonance at 350 MHz, this antenna cannot be a CPd radiator. The difference between the co-polar and cross-polar shown in Fig. 5.7 is more than 37 dB, which indicates that this antenna produces linear polarized waves. Since we were looking for an antenna to be used for communication through space, CP is a required characteristic for the antenna. Therefore we considered other designs.

5.5 Miniaturization

Demand for applying miniaturization techniques has stemmed from the need for power-efficient designs, cost-efficient designs, mobile and portable communication devices with limited allowable surface area for the antenna, and antennas that work in the VHF or

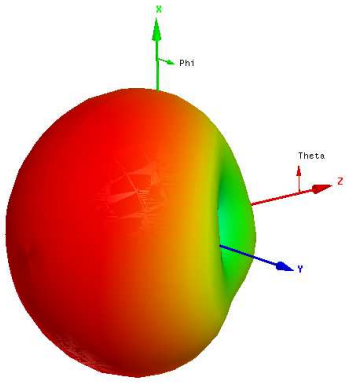

Fig. 5.5: Radiation gain of the rectangular slot antenna.

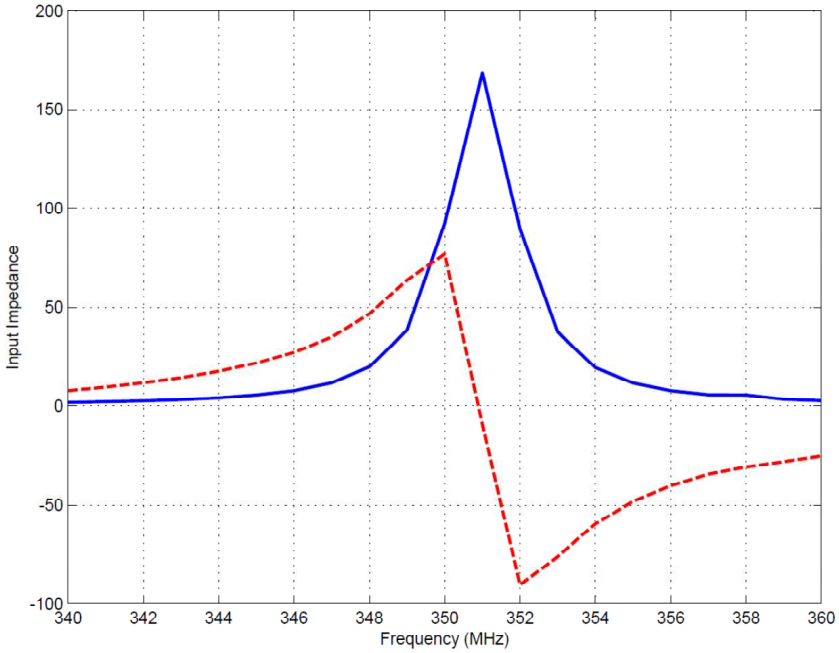

Fig. 5.6: Input impedance of the rectangular slot antenna.

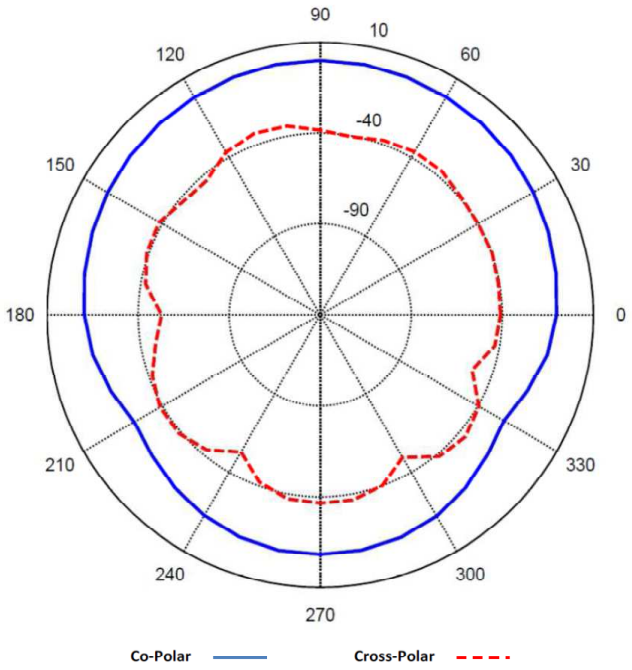

Fig. 5.7: Co-polar and cross-polar directivity components of the rectangular slot antenna.

UHF band. Study on the topic of antenna miniaturization has a relatively long history. Fundamental limitations of the small antenna are enumerated by Wheeler [8] and Chu [15]. Wheeler states that the small antenna is an antenna whose maximum dimension is less than a $\frac{1}{2\pi}$ wavelength. Chu used an arbitrary, small omnidirectional antenna in a sphere and an equivalent circuit model and derived the Q factor, which is the ratio of the stored energy to the radiated power. He showed that the calculated Q is a function of the radius of the sphere or the largest dimension of the antenna and interpreted it as a reciprocal of the fractional bandwidth. Harrington, Wheeler, Collin, and Hansen followed with studies on the topic of the limitations of small antennas [9, 30–32]. Harrington has shown that the gain of a small antennas is bounded and expressed by (5.1):

$$G = (ka)^2 + (ka)\,, \tag{5.1}$$

where k is $\frac{2\pi}{\lambda}$(radians/meter) and a is the radius of the sphere enclosing the maximum dimension of the antenna (meter). From all these studies, one can conclude that the smaller the maximum dimension of an antenna, the higher its Q, which has an inverse relation with bandwidth, meaning a lower bandwidth. So a trade-off between an antenna's radiation characteristics such as impedance bandwidth, efficiency, radiation gain, and antenna dimension is inevitable.

The miniaturization usually is achievable through two methods: by use of a dielectric with high permittivity material for the antenna [33] and by use of a special antenna [10, 11, 13, 34]. An antenna can have a reasonable impedance bandwidth when a dielectric with a high permittivity constant is used for the antenna size reduction [33]. Generally, using a high permittivity dielectric has the disadvantage of causing low-efficiency radiation due to the high impedance difference between the dielectric and air surrounding the antenna, which causes most of the electromagnetic energy to be trapped in the near field [35]. Also, the impedance matching of the antenna is more difficult in a high permittivity dielectric because it has low characteristic impedance. One way to improve the far field radiation when high permittivity material is used for the antenna dielectric is externally perforating the substrate by cutting an array of small holes in it. This decreases the effective permittivity but does not decrease the impedance bandwidth [36]. However, the position of the holes in the substrate can affect the radiation pattern.

Some studies about the use of the special antenna topology as the other miniaturization method have been done and a brief review of them follows. Given an understanding of the form of the magnetic current distribution on the slot and its boundary conditions in conjunction with the Maxwell's equations, the slot antenna is terminated with two series inductances which can satisfy the boundary conditions [13]. To make the antenna more compact, the inductor parts are in the form of coiled slot lines, and as a result the overall antenna dimension is about $0.05\lambda \times 0.05\lambda$. However, because the current density is increased on the smaller area of the dielectric, it faces more ohmic loss, and as a result the antenna efficiency and gain are all reduced by compacting the antenna. Also as mentioned previously,

the decrease in antenna size decreases the impedance bandwidth as well.

Placing the array of short circuited narrow slot-lines as a series of inductances vertical to the main slot as another technique for antenna miniaturization has been studied previously [10]. These perpendicular slits force the parallel component of the electric current to circulate around them. Therefore, this current, which determines the resonant frequency, traverses a longer path and as a result frequency decreases.

For a cavity-backed slot antenna, Hong etal. have presented a method for size reduction of the ground [11]. The metallic ground is replaced by parallel metal strips; these strips allow the perpendicular component of the electric currents to the slot to circulate. Eventually the straight strips were replaced by some meandered strips, reducing the size of the antenna. However, the drawback of this method is that decreasing the number of strips reduces efficiency and bandwidth because strips are paths for currents and the limited number of paths does not allow the currents to radiate efficiently.

One improving method for the impedance bandwidth of the miniaturized slot antenna has been discussed by Behdad and Sarabandi [10]. By using mutual coupling between two similar miniaturized slot antennas that are placed close to each other to create double resonant frequencies, the bandwidth of the structure is improved compared to one single antenna.

First and second iterations of Sierpinsky space-filling curves and Minkowski fractal slot antennas are proposed and compared by Moselhy and Ghali [34]. It is concluded that although by increasing the iteration of these two types of antennas they would be more compact, due to the higher coupling between slot parts the impedance bandwidth and gain are decreased.

By creating a fictitious short circuit and open circuit, it is possible to reduce the half wavelength slot antenna to the quarter wavelength slot antenna for further miniaturizing the antenna [12]. The idea of creating an open circuit at one end comes from the fact that a quarter wavelength spiral slot antenna shorted at one end acts like an open. It is noted that spiral slot antenna is not an efficient radiator because opposing equivalent magnetic

currents contribute to far field radiation and they tend to cancel each other.

Presented here are some general observations about the radiation characteristics of the miniaturized antennas. First is the limited impedance bandwidth, which was mentioned before. The other observation is bounded gain [30]. In a finite ground plane, because the magnetic currents in the upper and lower sides of the ground plane are in opposite directions, by decreasing the ground plane size, gain decreases as well; however, because of the presence of the dielectric, perfect cancelation does not occur [12]. In an infinite ground plane these upper and lower magnetic currents are decoupled. Also, back radiation is higher for the antenna on the smaller ground. Antenna efficiency can be a function of the size of the ground plane and the width of the slot [12]. By decreasing the ground size as mentioned before, the electric currents' density goes up, and as a consequence ohmic loss increases, which causes lower antenna efficiency. By narrowing the slot, the density of the parallel component of the electric currents near the edge of the slot increases; thus, the ohmic loss for this component goes up [12]. The other constraint about miniaturized antennas is their polarization [13]. When the size of the antenna compared to a wavelength is very small, the polarization is linear because phase shift between two perpendicular components of the magnetic current cannot be achieved.

Following the above literature review about miniaturization techniques and their inherent limitations, two different miniaturized structures mentioned above are presented below. Their results are in agreement with those aforementioned observations.

5.6 Miniaturized Slot Antennas

5.6.1 Spiral Slot Antenna

The first structure is similar to the Alford slot antenna with extended wings, or, one can say, it is similar to the four-arm spiral slot antenna. This antenna occupies a total space of $92\,mm \times 94\,mm$ and is fed with an L-shaped stripline feed. To have a better view of the antenna, its 3-D view on the 3U satellite is shown in Fig. 5.8. This antenna is placed on less than one third of a 3U cube surface area and resonates near a frequency of 359 MHz

(Fig. 5.9), but as expected, the efficiency is as low as 42% and the maximum gain is as low as 0.04 dB (Fig. 5.10). The other drawback for the use of this antenna for a space communication application is its linear polarized radiation, which as mentioned before, it is a characteristic of the miniaturized class.

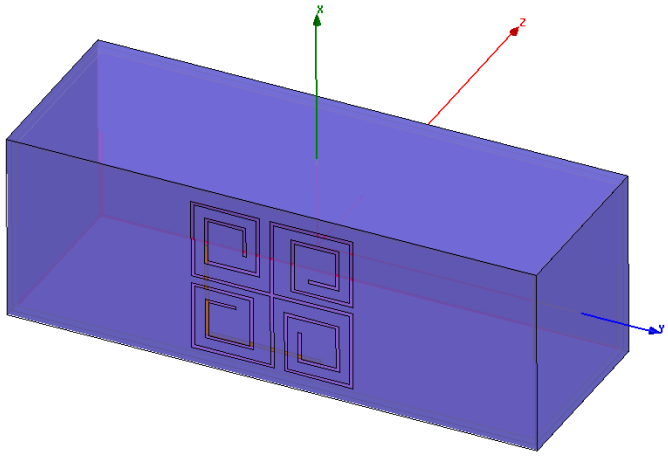

Fig. 5.8: Spiral slot antenna on 3U CubeSat.

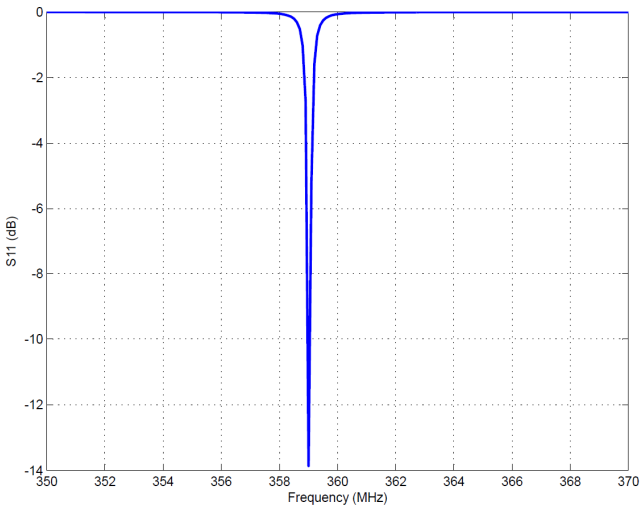

Fig. 5.9: Return loss of the spiral slot antenna.

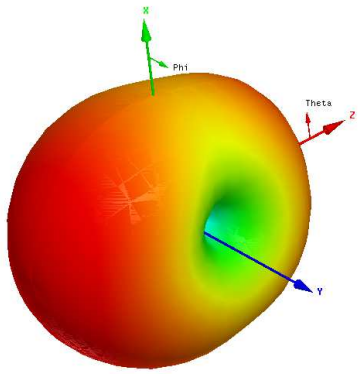

Fig. 5.10: 3-D radiation pattern of the spiral slot antenna.

5.6.2 Fractal Slot Antenna

The other antenna topology studied is a fractal shape slot antenna. Two fused quartz substrates each with 4 mm thickness were chosen for the antenna, and one stripline feed was placed between two substrates to feed the antenna. The total substrate thickness is 8 mm in order to cause further size reduction. The overall size of the rectangular space occupied by this antenna is 112 $mm \times 114\,mm$. 112 mm is larger than one dimension of the 3U CubeSat and it is acceptable because all dimensions of the satellite can have small tolerance. If we place a simple rectangular slot antenna on this space, it radiates near a frequency of 480 MHz. By adding some meander parts to increase the slot length and to make some parts of the antenna be further from the edges as is shown in Fig. 5.11, we reach a resonant frequency of 379 MHz (Fig. 5.12) with 3.9 dB gain (Fig. 5.13) and the fractional impedance bandwidth of 0.08%. We reduced the frequency by 100 MHz while the reduction in the antenna radiation gain was only around 1 dB. Simulations show that the efficiency is deteriorated by 6%.

5.6.3 Fractal Slot Antenna Array

We placed a two-element array of fractal shape slot antennas (Fig. 5.14) to see whether we could improve the antenna specifications, but we do not expect much improvement because there is limited space between the elements. When the distance between two

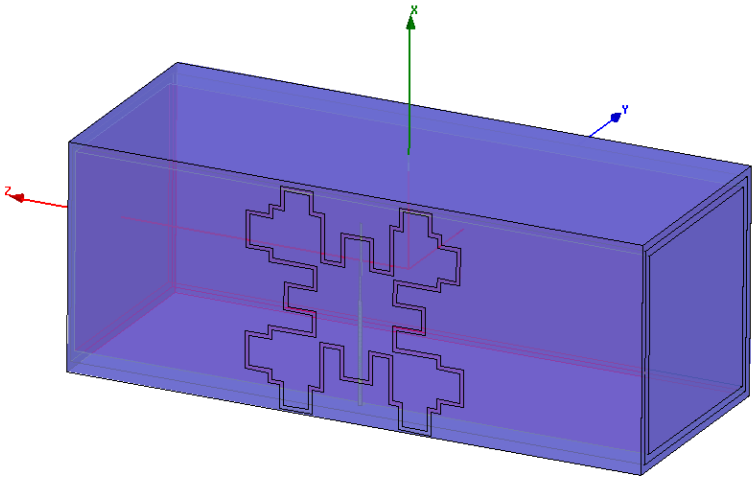

Fig. 5.11: Fractal slot antenna on 3U CubeSat.

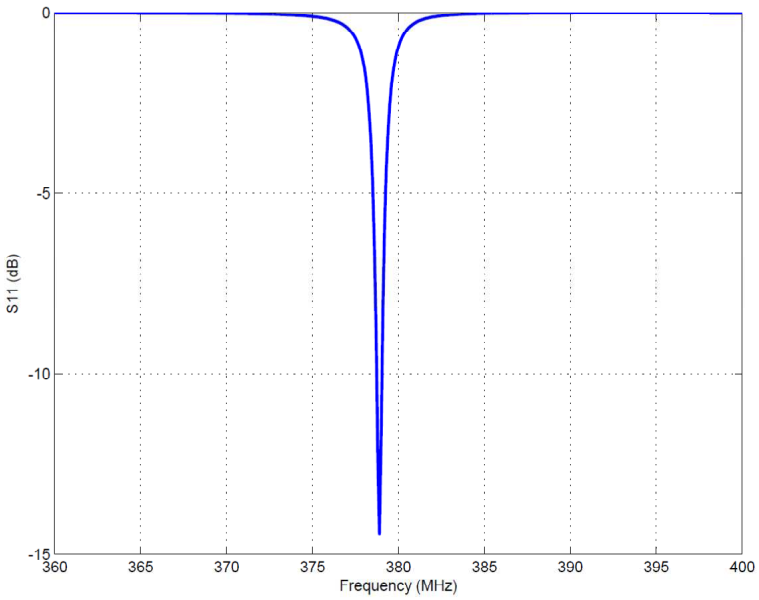

Fig. 5.12: Return loss of the fractal slot antenna.

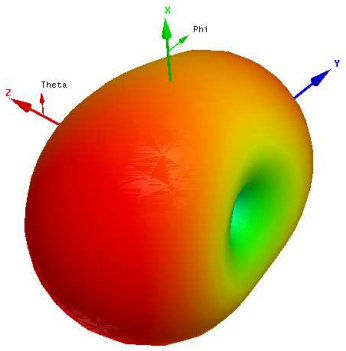

Fig. 5.13: 3-D radiation pattern of the fractal slot antenna.

antennas is $130mm$, the resonant frequency decreases to 362 MHz, and bandwidth and gain would reduce as well to values even less than those of a single antenna. If we increase this distance to $140mm$, the resonant frequency increases to $364\,MHz$ and the gain improves by just less than $0.1\,dB$.

It is expected that by further increasing the distance between two elements, the frequency increases to the frequency of a single antenna. Also, radiation gain and bandwidth can be improved to some extent, but $140\,mm$ distance is almost the largest possible distance between two elements because it is not efficient to place the elements near the edges as it destroys the currents distribution. The polarization of the antenna as expected is linear and the difference between co-polar and cross-polar components at the direction of maximum radiation is more than $40\,dB$.

5.7 Design Procedure of the Circularly Polarized Slot Antenna for the First Posture of 3U CubeSat in Orbit

To achieve the CP, the vertical and horizontal components of the electric field should have the same strength while one component leads the other component by one quarter of a wave length. For this condition either we have to use two individual linear polarized antennas where each of them can produce an electric field in a direction perpendicular to

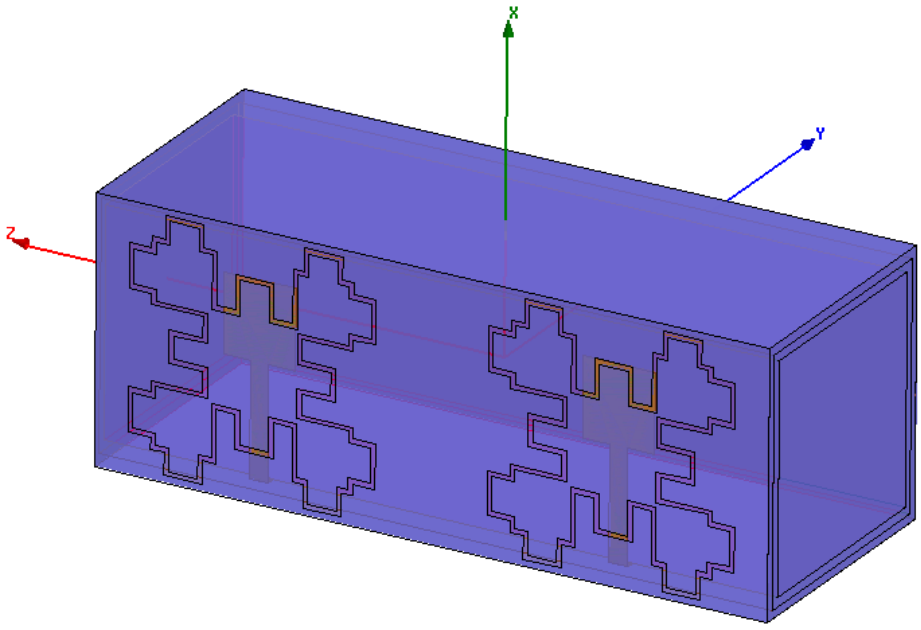

Fig. 5.14: Fractal slot array antenna.

the other antenna's electric field and with the same strength or use the special topologies like square- or circular-shape antennas. If, for example the rectangular shape is used, the manner of feeding should excite the antenna such that the magnitude of the currents on each side be proportional to the length of that side [2]. For the first posture of the satellite toward the earth (Fig. 5.15), we placed a square slot antenna with total length of 432 mm fed by a stripline. This antenna resonates at a frequency of 407 MHz with 5 dB gain and 88% efficiency at this frequency. Looking to the horizontal and vertical components of the directivity (Fig. 5.16), we noticed that the difference is more than 24dB and the polarization of the antenna is linear at $phi = 40$ degrees. We guessed that by adding another stripline feed to excite one of the perpendicular sides and making a 90 degree phase shift between the two feeds, CP could be achieved. When we added the second feed with a 90 degree phase shift (Fig. 5.17), the resonant frequency dropped to 400 MHz with 5 dB AR. This AR value shows we can improve it to even less than 3 dB by some modifications, but before that we thought about how we could improve the gain and reduce the frequency.

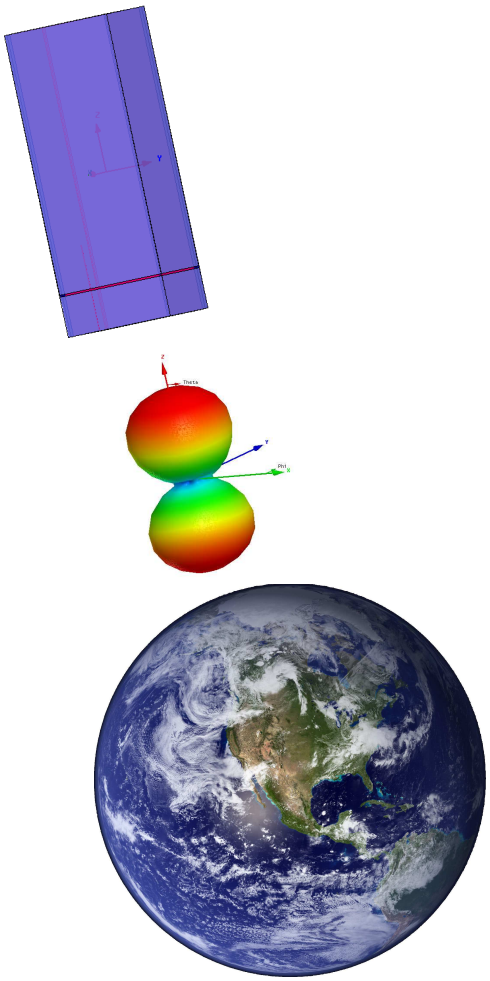

Fig. 5.15: Square slot antenna on the 3U CubeSat (earth image from www.csufresno.edu).

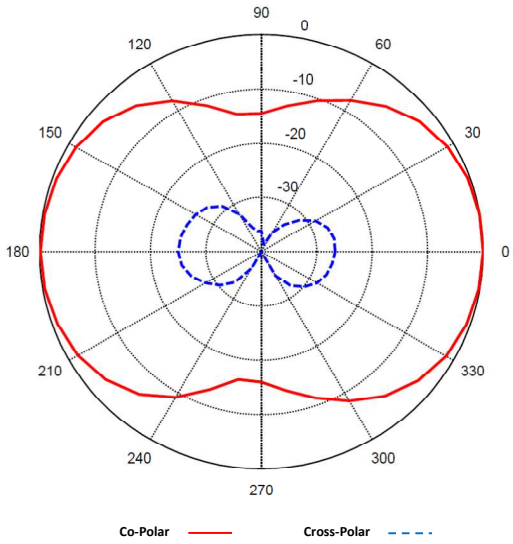

Fig. 5.16: Radiation pattern of the square slot antenna on the 3U CubeSat.

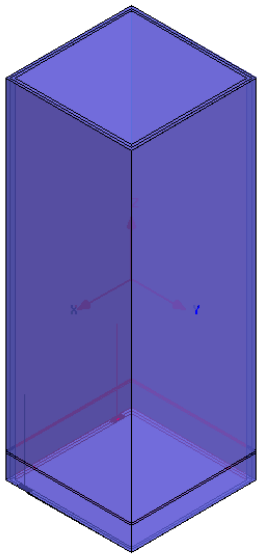

Fig. 5.17: Square slot antenna excited with two striplines in two sides.

5.7.1 Frequency Reduction and Gain Enhancement by Adding Parasitic Square Slots

Similarly to the Yagi-Uda antenna, which has some directive and reflective dipoles, we considered adding another slot to act as a reflector. We placed one square slot antenna at 130 mm (around one sixth of a wavelength) above the main square slot antenna with no excitation for it (Fig. 5.18). Because of the small distance between main slot and the parasitic slot, current distribution changes such that it seems the effective slot antenna length is increased and as a result the frequency is reduced to 381 MHz. Also, radiation gain increases slightly to 5.13 dB with 83% radiation efficiency. We increased the distance between the main slot and the parasitic slot to 170 mm, less than a quarter wavelength, to see how it would affect the antenna performance. Simulation shows the frequency is reduced by 1 MHz to 380 MHz, and we can say that moving the parasitic slot further away almost does not change the resonant frequency but gain and antenna efficiency are enhanced to 5.34 dB and 87%, respectively. If we increase the distance to 180 mm, although the frequency again drops by 1 MHz to 379 MHz the antenna radiation gain decreases to 4.56 dB, and we can say that 170 mm is the optimum distance between the antenna and one parasitic slot. For additional clarification, these mentioned values are shown in Table 5.1.

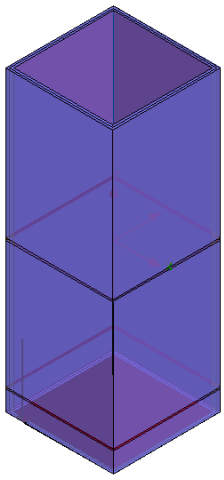

Fig. 5.18: Square slot antenna with one parasitic square slot.

Then we added one more parasitic slot to see whether it could make an improvement (Fig. 5.19). By performing some individual simulations we found out that adding one more parasitic can improve the gain and even AR when we excite the antenna with two stripline feeds. Also, it helps us to reduce the resonant frequency but it should not be too close to the first parasitic. Therefore, we would need some optimizations to choose the right positions for the slots after we reach our target resonant frequency.

Table 5.1: Effect of the parasitic square slot at different distances to the main square slot antenna.

Case	Resonant frequency (MHz)	Gain (dB)	Efficiency (%)
No parasitic	407	5	88
One parasitic in 130mm	381	5.13	83
One parasitic in 170mm	380	5.34	87
One parasitic in 180mm	379	4.56	92

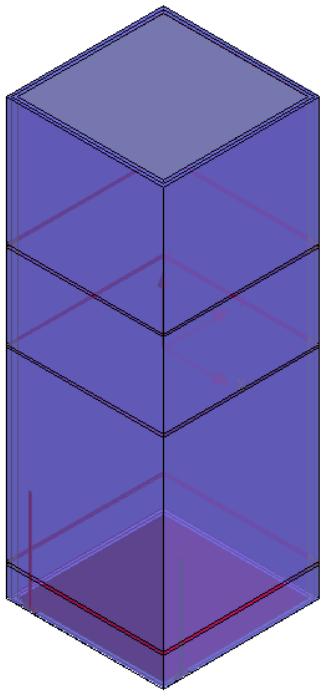

Fig. 5.19: Square slot antenna with two parasitic square slots.

5.7.2 Gain Enhancement with Built in Structure Metal Reflectors

One way to increase the antenna gain can be built-in metal wings working as reflectors for the antenna. It means that after the satellite reaches orbit, these metal reflectors pop up as shown in Fig. 5.20.

We performed some simulations to study the effect of the reflector's size on the radiation gain. The results are compared in Table 5.2 and they explicitly show that the optimum size of the reflector to achieve the maximum radiation gain is 100 mm.

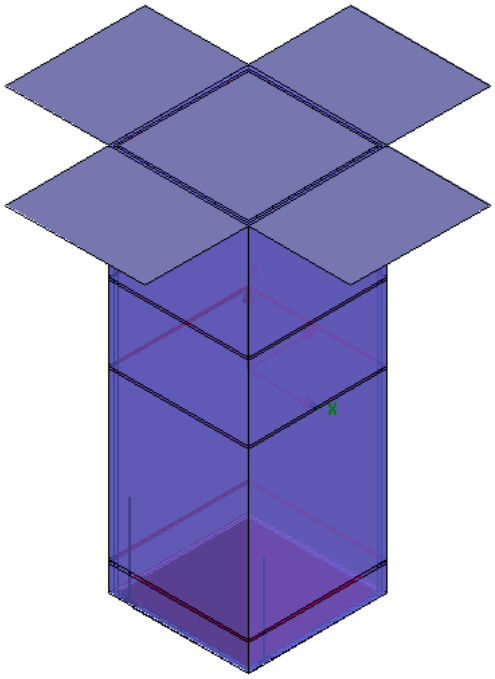

Fig. 5.20: Metal reflectors on the 3U CubeSat.

Table 5.2: Effect of the reflector's size on the antenna's radiation characteristics.

Reflector's size (mm)	Resonant frequency (MHz)	Gain (dB)	AR (dB)
80	378.4	7.17	1.72
100	378.2	7.7	1.4
130	378.1	7.4	0.7
300	378.4	6.76	1.12

5.7.3 Final Antenna Geometry for Target Frequency

For additional frequency reduction we increased the length of the slot antenna by adding eight extra lines totaling 264 mm to the square antenna on four sides (Fig. 5.21). Therefore, the total length of the slot antenna was 695 mm. After optimizing the distance between the main slot and two parasitic slots, we placed the first and second parasitic slots 120 mm and 180 mm away from the main slot, respectively. Both stripline feeds placed on perpendicular sides have 80 mm length and 1 mm width and are matched to the 50 Ω coaxial cable. This new meandered slot antenna resonates at a frequency of 352 MHz with 4 dB gain and 88% efficiency at this frequency. The return loss of the antenna is shown in Fig. 5.22. Currents in opposite directions which circulate around these counterpart lines are responsible for the gain reduction. The AR at this resonant frequency is 1.8 dB (Fig. 5.23).

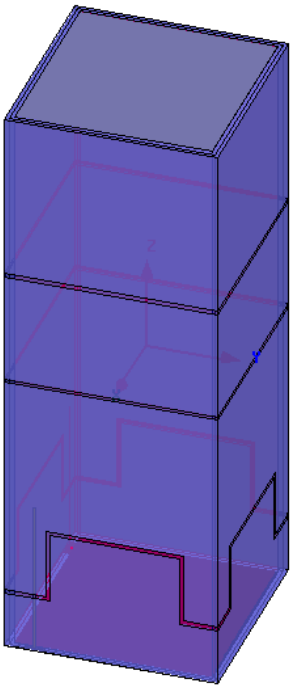

Fig. 5.21: CPd meandered square slot antenna on the 3U CubeSat.

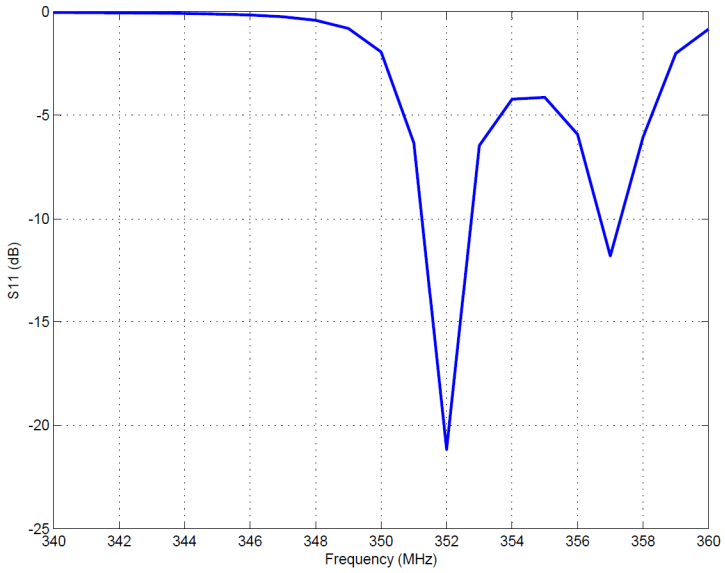

Fig. 5.22: Return loss of the meandered square slot antenna on the 3U CubeSat.

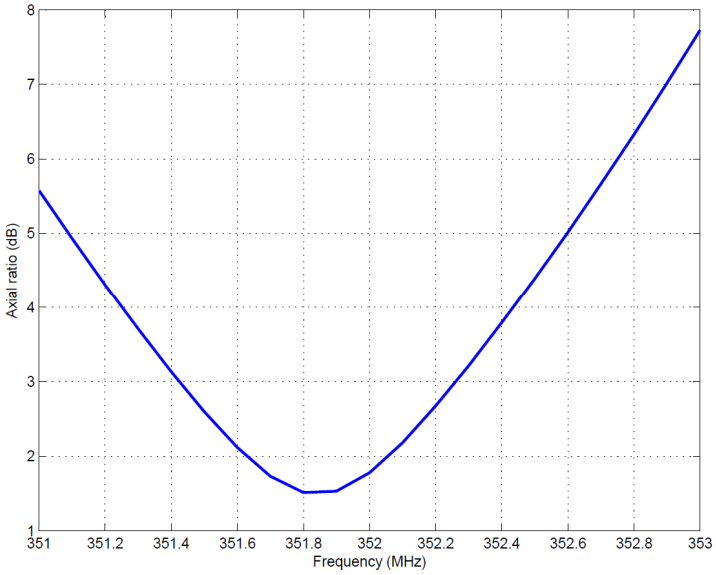

Fig. 5.23: AR of the meandered square slot antenna on the 3U CubeSat.

We can better understand the effect of the second parasitic slot by removing one of the parasitic slots. The results show the frequency, gain and AR all increase to $359 MHz$, $4.27 dB$ and $8.4\ dB$, respectively. However, if the AR were our main concern and to decrease the frequency we were to increase the length of the meandered slot, the gain would be reduced from $4.27\ dB$. So the importance of the second parasitic slot is clear. The comparison is shown in Table 5.3. Final structure of the antenna shown in Fig. 5.24 has four reflectors, each with size of $100\ mm$. The antenna resonates at a frequency of $352\ MHz$ with the radiation gain of $6.8\ dB$ and AR of $1.8\ dB$.

5.8 Design Procedure of the Circularly Polarized Slot Antenna for the Second Posture of the 3U CubeSat in Orbit

For the second pose of the 3U CubeSat in orbit aimed toward the earth shown in Fig. 5.25, to design a slot antenna working around a frequency of $350\ MHz$ with CPd radiation as the main concern, we thought about two different antenna topologies, each of which is linearly polarized but the overall structure radiates CPd waves.

5.8.1 Meandered Rectangular Slot Antenna on 3U CubeSat

We picked a rectangular slot as one of the linearly polarized antennas. We used two fused quartz substrates with a total thickness of $8\,mm$ for the antenna dielectric and excited it with a stripline feed placed between two substrates. In one of the previous sections we stated that the size of the rectangular slot antenna for this frequency should be $90\ mm \times 225\,mm$. This size occupies a large area on the satellite and if we place another antenna on the CubeSat, the small distance between the two antennas disfigures the natural current distribution around each of the antennas and the resulting radiation pattern. Therefore, we miniaturized it by increasing the dielectric thickness to a total of $8\ mm$ and by adding some meander parts to the slot antenna to occupy a $145\ mm \times 90\ mm$ area (Fig. 5.26).

Table 5.3: Effect of the number of the parasitic slot on the meandered square slot antenna's radiation characteristics.

Case	Resonant frequency (MHz)	Gain (dB)	AR (dB)
Two parasitic slots	352	4	1.8
One parasitic slot	359	4.27	8.4

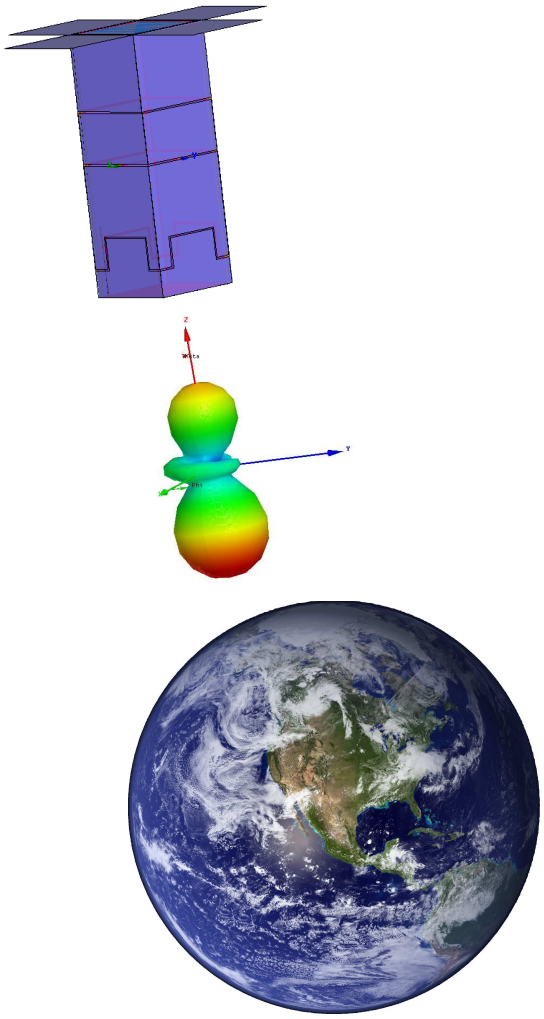

Fig. 5.24: Final structure of the CPd slot antenna on the 3U CubeSat.

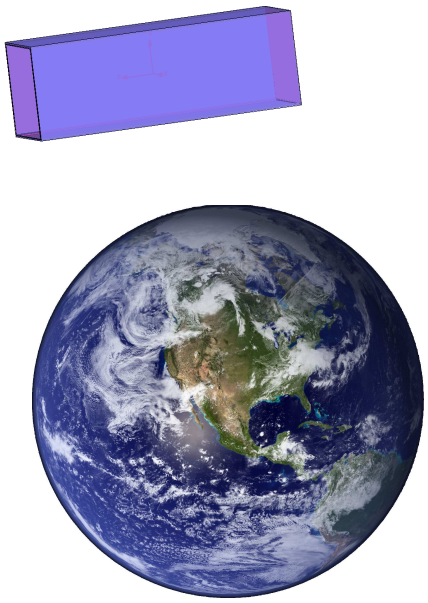

Fig. 5.25: Second pose of the 3U CubeSat in orbit toward the earth.

To match this antenna with the $50-\Omega$ coaxial cable, it is fed with a stripline designed to have two parts. The first part, attached to the port, has $45\,mm$ length and $2\,mm$ width and then it is extended by narrower part with a length of $20\,mm$ and width of $1\,mm$. This antenna resonates at a frequency of $352\,MHz$. Looking at the vertical and horizontal directivity components shown in Fig. 5.27, one can notice that the value of the horizontal directivity component (phi-component) is around $30\,dB$ more than the vertical directivity component (theta-component) at the maximum radiation direction ($\theta = 90$ degrees and $\phi = 270$ degrees) which is a direction toward the earth; it means this antenna is linearly polarized.

Now if we design the second antenna in which the maximum value of its radiation component in the theta plane will be equal to the maximum value of the first antenna's radiation pattern in the phi plane while they have a 90 degree phase shift, the resulting waves should be CPd waves.

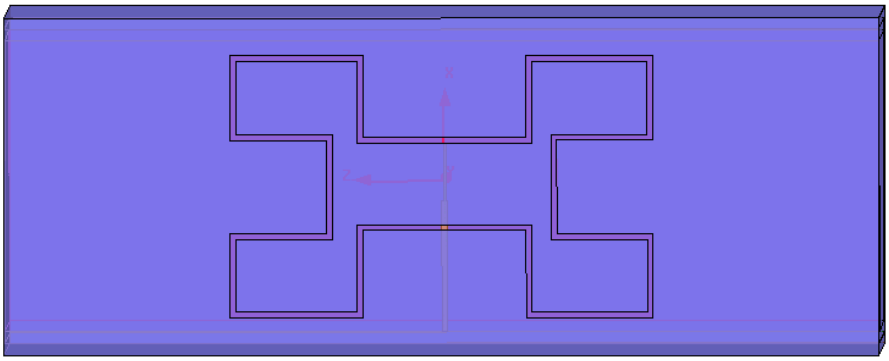

Fig. 5.26: Front view of the meandered rectangular slot antenna.

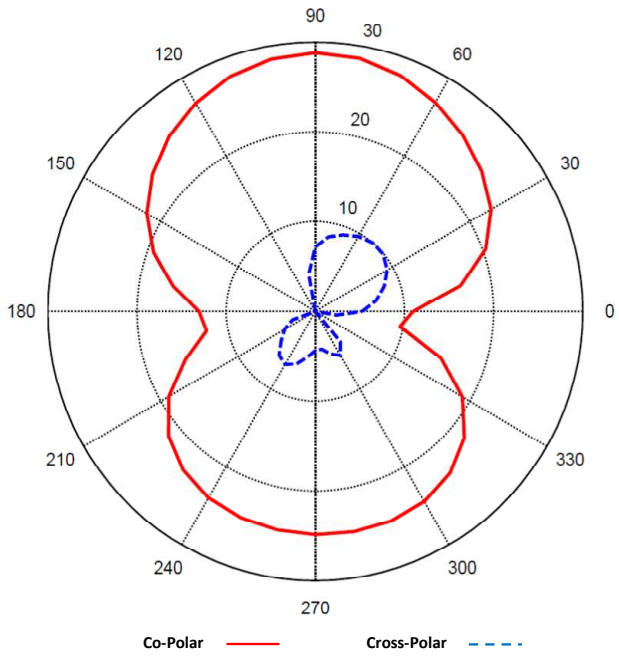

Fig. 5.27: Radiation pattern of the meandered rectangular slot antenna on the 3U CubeSat at its resonant frequency.

5.8.2 Horseshoe-Shaped Slot Antenna on the 3U CubeSat

Shown in Fig. 5.28, we designed a horseshoe-shaped slot antenna on three sides near one end of the satellite to find its resonant frequency. Similar to what we used for the first antenna, again we used two fused quartz substrates with a total thickness of 8 mm and excited the antenna with a wave port on the satellite's surface which faces toward the earth to have its maximum radiation in this direction. This antenna resonates at a frequency of 475 MHz.

To reduce the resonant frequency we increased the antenna length by adding two extra symmetric slots perpendicular to the horseshoe shape on two opposite lateral sides (Fig. 5.29). These slots are vertical to the main slot and they simply force the electric currents to circulate around them to reduce the frequency and they do not significantly reduce the radiation gain. To excite this new antenna we used a stripline feed between two dielectric substrates. The total length of the antenna with the inclusion of two additional slots of 110 mm length each, is 695 mm, and it resonates at a frequency of 350 MHz with a maximum radiation gain of 3.47 dB. If we look at the directivity components at the resonant frequency shown in Fig. 5.30, one can easily find that the slot antenna is linearly polarized and the value of the vertical component (theta component) is more than the horizontal component (phi component). The fractional impedance bandwidth is 0.57% and it is observed that if we decrease the dielectric thickness to half of what it is now, to have the same resonant frequency we have to increase the slot length by 30 mm. Also a reduction in dielectric thickness decreases the fractional impedance bandwidth to 0.28%.

Now we expect that if we combine two antennas on one satellite and excite them with a 90 degree phase shift, we achieve CPd radiation. We know that the distance between two antennas has an effect on the resonant frequency and the value of the AR. We also expect the coupling between two antennas to reduce the overall radiation gain.

5.8.3 Combining Two Linear Polarized Slot Antennas to Achieve the Circularly Polarized Radiation

We placed two antennas on the satellite's surface, each one as much as possible near

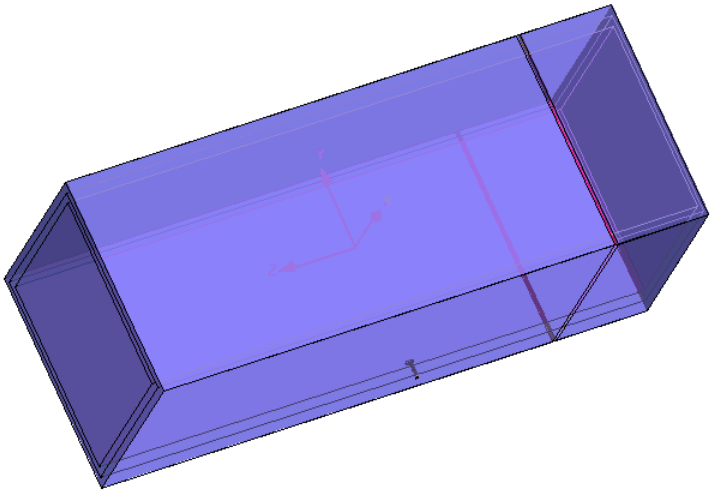

Fig. 5.28: Horseshoe-shaped slot antenna on the 3U CubeSat.

the opposite end (Fig. 5.31). The least distance between the two antennas is 109 mm. Because of the coupling effect between the antennas, to reach a resonant frequency near 350 MHz, the horseshoe-shaped antenna length can be decreased by 54 mm to 641 mm. Due to the coupling between both antennas we should again adjust their stripline feeds to match each antenna with the $50 - \Omega$ coaxial cable. The feed of the horseshoe-shaped slot has 70 mm length and 1 mm width, and the feed of the meandered rectangular slot consists of two parts: the first part, which is attached to the port, has 80 mm length and 2 mm width and the second part as a continuation of the first part has 15 mm length and 4 mm width. Both antennas resonate at the center frequency of 353.1 MHz with 97% radiation efficiency and 2.47 dB gain at $\phi = 270$ degrees and $\theta = 90$ degrees, which is in the direction toward the earth. Both antennas have more than 10 dB return loss in the frequency band of 352.7 MHz to 353.5 MHZ. The meandered rectangular slot antenna return loss and the horseshoe-shaped slot antenna's return loss are shown in Fig. 5.32 and Fig. 5.33, respectively.

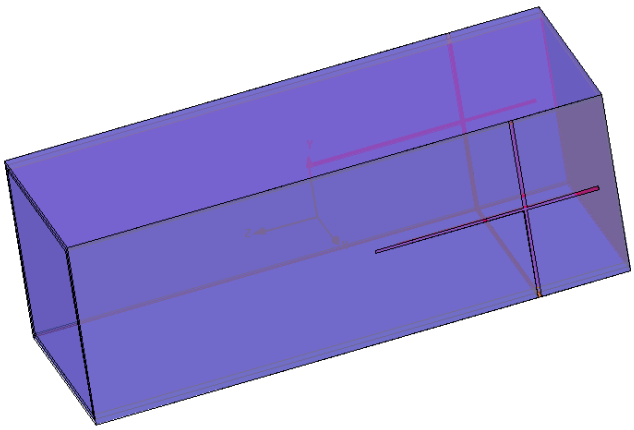

Fig. 5.29: Increased length of the horseshoe-shaped slot antenna with two extra slots on the 3U CubeSat.

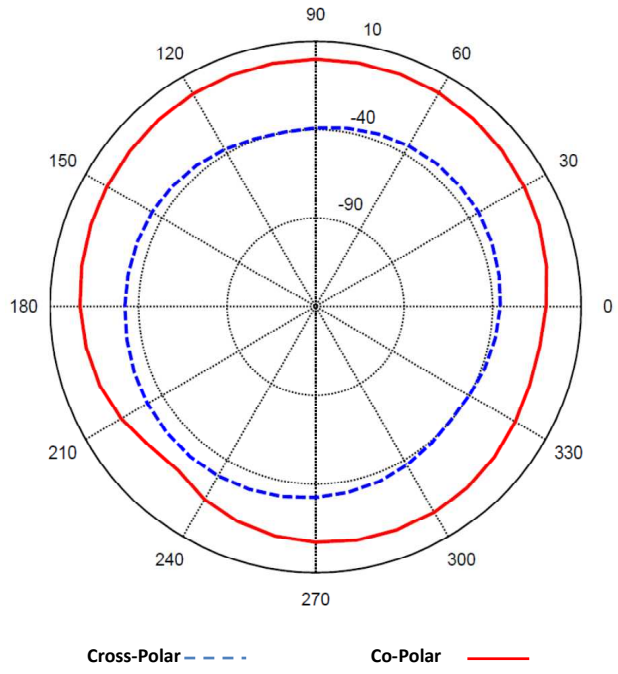

Fig. 5.30: Radiation pattern of the horseshoe-shaped antenna on the 3U CubeSat at its resonant frequency.

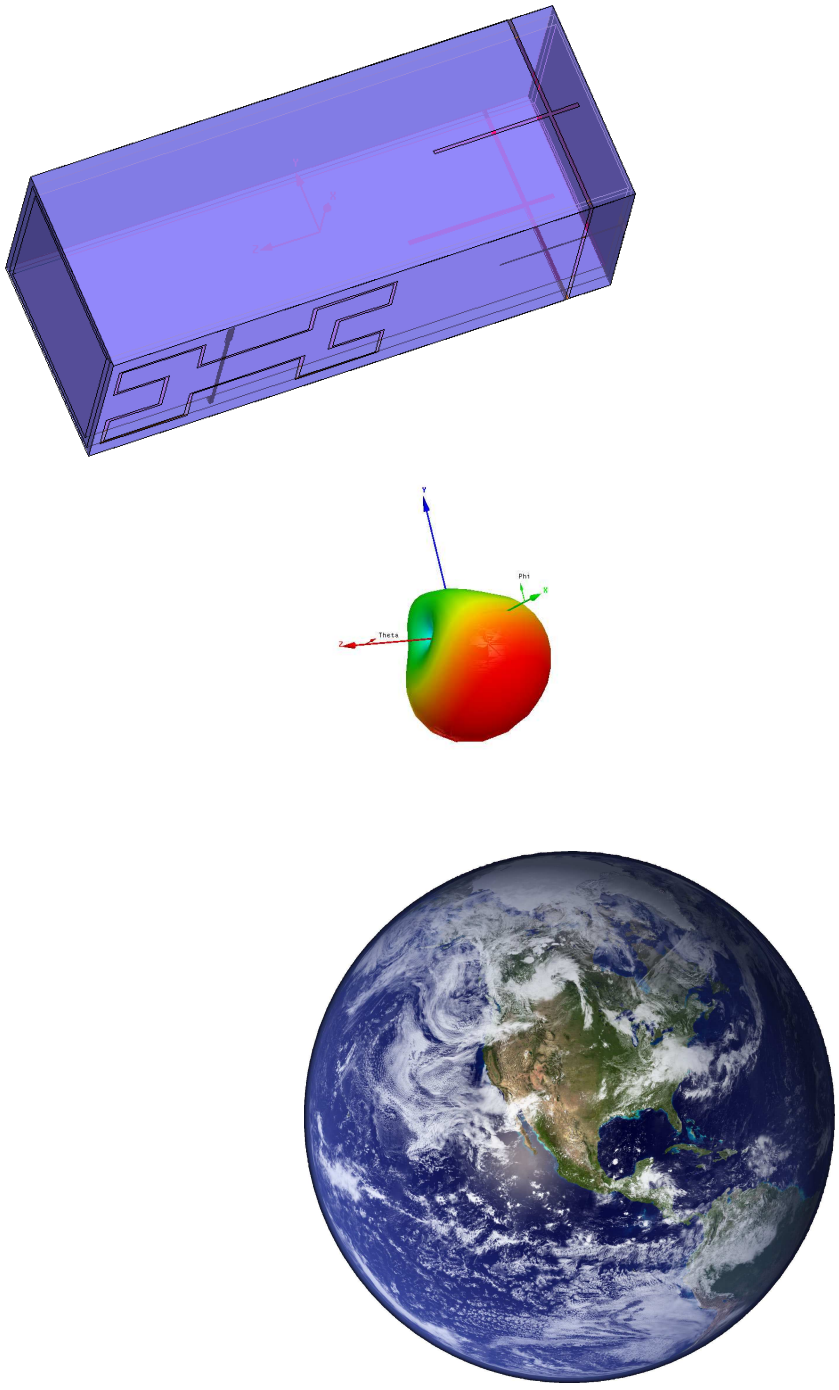

Fig. 5.31: Two different slot antennas on the 3U CubeSat radiating toward earth.

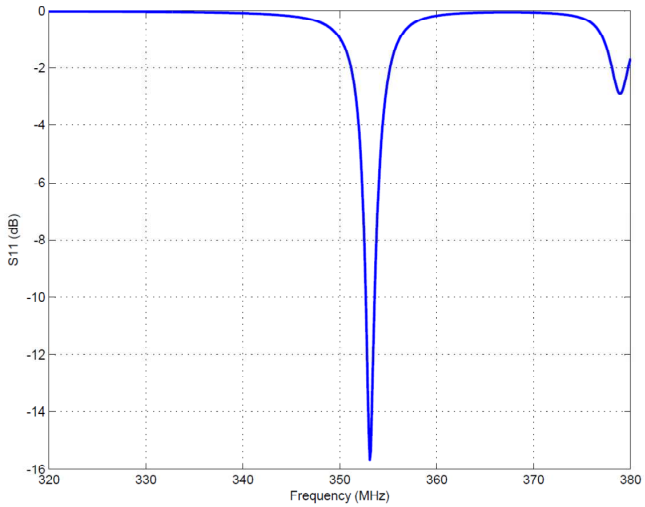

Fig. 5.32: Meandered rectangular slot antenna return loss.

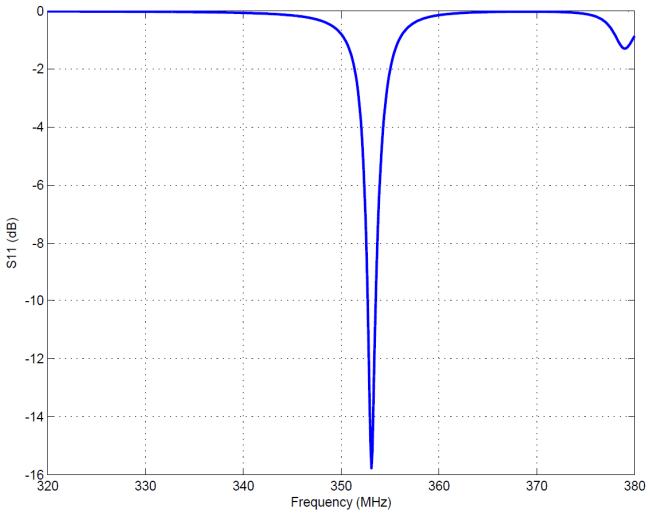

Fig. 5.33: Horseshoe-shaped slot antenna return loss.

5.8.4 Circular Polarization Technique

By exciting both antennas with equal power and a 90 degree phase shift, the lowest AR value in the frequency band was 4 dB, so we expected that if we excite them with different power levels, we may achieve the AR better than 3 dB. In simulation we can simply set different values for the sources, but for the fabrication design we can use a power divider. The minimum AR value is 0.8 dB if we excite the meandered rectangular shape antenna with a double power level. The reason for using different power levels for excitation stems from the difference between the dominant gain component of each antenna; the co-polar component of the meandered rectangular shape is not as strong as the co-polar component of the second antenna. By performing a couple of simulations, we reached the minimum 0.5 dB AR if we increased the 90 degree phase shift to a 100 degree phase shift. However, with the 90 degree phase shift we still had good CPd radiation. The AR with a 90 degree phase shift is shown in Fig. 5.34.

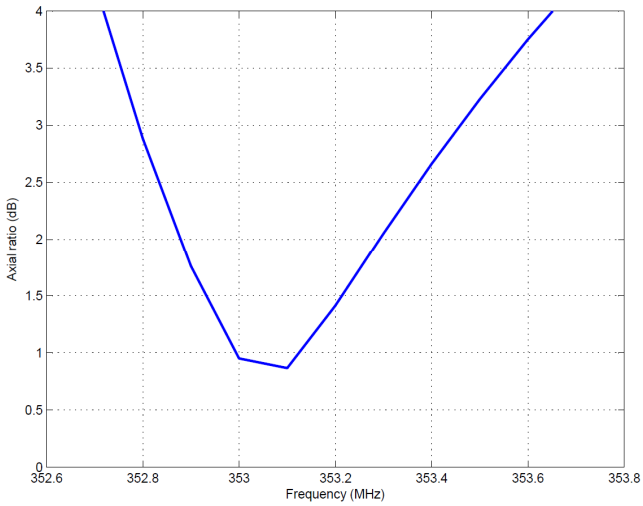

Fig. 5.34: AR of the combined slot antennas on the 3U CubeSat.

Chapter 6

Summary and Future Work

In this research we first studied the effect of the ground size on the impedance bandwidth and directivity of the slot antenna and we concluded that with the smaller ground size, the antenna has less bandwidth and directivity. Also, we found that for the cavity-backed slot antenna, the size of the cavity has a major effect on the resonant frequency, bandwidth, and efficiency of the antenna. These results helped us better understand the challenges we confronted later in the slot antenna miniaturization. The second part of our work was about the design and fabrication of the CPd stripline-fed cavity-backed cross slot antenna and its two-element array. The fabrication results of the single slot were very close to the simulation results, but for the array antenna, fabrication results were not very close to its simulation results due to the low accuracy of the fabricated prototype. We also compared the performance of two feeding methods including the coaxial probe and stripline feed for achieving CPd radiation. The other part of the research was designated to describe the design and fabrication of the CPd patch antenna with the specific dimensions to compare its performance with a commercial patch antenna. The results confirmed that our lab-design patch antenna had superior performance over the commercial one and was also cheaper. In the last part of our work we faced the challenges of miniaturization techniques for a slot antenna on the smaller ground plane compared to the antenna size. We designed two high-gain CPd slot antenna structures working in the UHF band for a 3U CubeSat.

For future work, a power divider and phase shifter circuit can be designed for the second UHF antenna structure. The designed UHF slot antennas can be fabricated with proper facilities since their fabrications need high precision. Also, finding appropriate methods for improving the radiation gain and impedance bandwidth of a miniaturized slot antenna can be subjects of future studies.

References

[1] M. N. Mahmoud, "Integrated solar panel antennas for cube satellites," Master's thesis, Utah State University, Logan, UT, 2010.

[2] C. A. Balanis, *Antenna Theory, Analysis, and Design.* Hoboken, NJ: John Wiley and Sons, 2005.

[3] J.-S. Row, "The design of a squarer-ring slot antenna for circular polarization," *Antennas and Propagation, IEEE Transactions*, vol. 53, no. 6, pp. 1967–1972, June 2005.

[4] D. Sievenpiper, H.-P. Hsu, and R. Riley, "Low-profile cavity-backed crossed-slot antenna with a single-probe feed designed for 2.34-ghz satellite radio applications," *Antennas and Propagation, IEEE Transactions*, vol. 52, no. 3, pp. 873–879, Mar. 2004.

[5] K.-L. Wong, C.-C. Huang, and W.-S. Chen, "Printed ring slot antenna for circular polarization," *Antennas and Propagation, IEEE Transactions*, vol. 50, no. 1, pp. 75–77, Jan. 2002.

[6] D. M. Pozar, *Micrownve Engineering.* Hoboken, NJ: John Wiley and Sons, 2005.

[7] C. Allen, A. Eldek, A. Elsherbeni, C. Smith, C.-W. Huang, and K.-F. Lee, "Dual tapered meander slot antenna for radar applications," *Antennas and Propagation, IEEE Transactions*, vol. 53, no. 7, pp. 2324–2328, July 2005.

[8] H. Wheeler, "Fundamental limitations of small antennas," *Proceedings of the IRE*, vol. 35, no. 12, pp. 1479–1484, Dec. 1947.

[9] R. Hansen, "Fundamental limitations in antennas," *Proceedings of the IEEE*, vol. 69, no. 2, pp. 170–182, Feb. 1981.

[10] N. Behdad and K. Sarabandi, "Bandwidth enhancement and further size reduction of a class of miniaturized slot antennas," *Antennas and Propagation, IEEE Transactions*, vol. 52, no. 8, pp. 1928–1935, Aug. 2004.

[11] W. Hong, N. Behdad, and K. Sarabandi, "Size reduction of cavity-backed slot antennas," *Antennas and Propagation, IEEE Transactions*, vol. 54, no. 5, pp. 1461–1466, May 2006.

[12] K. Sarabandi and R. Azadegan, "Design of an efficient miniaturized uhf planar antenna," *Antennas and Propagation, IEEE Transactions*, vol. 51, no. 6, pp. 1270–1276, June 2003.

[13] R. Azadegan and K. Sarabandi, "Design of miniaturized slot antennas," in *Antennas and Propagation Society International Symposium, 2001. IEEE*, vol. 4, pp. 565–568 vol. 4, 2001.

[14] H. Booker, "Slot aerials and their relation to complementary wire aerials (babinet's principle)," *Electrical Engineers - Part IIIA: Radiolocation, Journal of the Institution*, vol. 93, no. 4, pp. 620–626, 1946.

[15] L. J. Chu, "Physical limitations of omni directional antennas," *Journal of Applied Physics*, vol. 19, no. 12, pp. 1163–1175, Dec. 1948.

[16] B. Zheng and Z. Shen, "Effect of a finite ground plane on microstrip-fed cavity-backed slot antennas," *Antennas and Propagation, IEEE Transactions*, vol. 53, no. 2, pp. 862–865, Feb. 2005.

[17] H. Morishita, K. Hirasawa, and K. Fujimoto, "Analysis of a cavity-backed annular slot antenna with one point shorted," *Antennas and Propagation, IEEE Transactions*, vol. 39, no. 10, pp. 1472–1478, Oct. 1991.

[18] S. Shi, K. Hirasawa, and Z. N. Chen, "Circularly polarized rectangularly bent slot antennas backed by a rectangular cavity," *Antennas and Propagation, IEEE Transactions*, vol. 49, no. 11, pp. 1517–1524, Nov. 2001.

[19] J. Huang, "A technique for an array to generate circular polarization with linearly polarized elements," *Antennas and Propagation, IEEE Transactions*, vol. 34, no. 9, pp. 1113–1124, Sept. 1986.

[20] Q. Li and Z. Shen, "An inverted microstrip-fed cavity-backed slot antenna for circular polarization," *Antennas and Wireless Propagation Letters, IEEE*, vol. 1, no. 1, pp. 190–192, 2002.

[21] J.-S. Row, C. Sim, and K.-W. Lin, "Broadband printed ring-slot array with circular polarisation," *Electronics Letters*, vol. 41, no. 3, pp. 110–112, Feb. 2005.

[22] Rogers Corporation, [www.rogerscorp.com].

[23] Nearfield Systems Inc., [www.nearfield.com].

[24] S. Vaccaro, C. Pereira, J. Mosig, and P. de Maagt, "In-flight experiment for combined planar antennas and solar cells (solant)," *Microwaves, Antennas Propagation, IET*, vol. 3, no. 8, pp. 1279–1287, Dec. 2009.

[25] K.-F. Tong and T.-P. Wong, "Circularly polarized u-slot antenna," *Antennas and Propagation, IEEE Transactions*, vol. 55, no. 8, pp. 2382–2385, Aug. 2007.

[26] P. Sharma and K. Gupta, "Analysis and optimized design of single feed circularly polarized microstrip antennas," *Antennas and Propagation, IEEE Transactions*, vol. 31, no. 6, pp. 949–955, Nov. 1983.

[27] Orban D. andMoernaut G.J.K., [www.orbanmicrowave.com].

[28] Space Dynamics Laboratory, [www.sdl.usu.edu].

[29] A. Khoshniat, "A linearly and circularly polarized active integrated antenna," Master's thesis, Utah State University, Logan, UT, 2011.

[30] R. Harrington, "Effect of antenna size on gain, bandwidth, and efficiency," *Journal of Research of the National Bureau of Standards*, vol. 64-D, pp. 1–12, Jan.-Feb. 1960.

[31] H. Wheeler, "Small antennas," *Antennas and Propagation, IEEE Transactions*, vol. 23, no. 4, pp. 462–469, July 1975.

[32] R. E. Collin, "The minimum q of small antennas (a discussion of recent controversies)," IEEE Toronto Section, Electromagnetics and Radiation Joint Chapter, 1998.

[33] R. Mongia, A. Ittibipoon, and M. Cuhaci, "Low profile dielectric resonator antennas using a very high permittivity material," *Electronics Letters*, vol. 30, no. 17, pp. 1362–1363, Aug. 1994.

[34] T. Moselhy and H. Ghali, "Design of fractal slot antennas," in *Microwave Conference, 2004. 34th European*, vol. 3, pp. 1265–1268, Oct. 2004.

[35] H. Mosallaei and K. Sarabandi, "Magneto-dielectrics in electromagnetics: concept and applications," *Antennas and Propagation, IEEE Transactions*, vol. 52, no. 6, pp. 1558–1567, June 2004.

[36] J. Colburn and Y. Rahmat-Samii, "Patch antennas on externally perforated high dielectric constant substrates," *Antennas and Propagation, IEEE Transactions*, vol. 47, no. 12, pp. 1785–1794, Dec. 1999.